

# Tracing Arctic precipitation changes in the North Atlantic Ocean

Selina Catherine Klemm

Master of Science Thesis



# Tracing Arctic precipitation changes in the North Atlantic Ocean

MASTER OF SCIENCE THESIS

For the degree of Master of Science in Water Management at Delft  
University of Technology

Selina Catherine Klemm

June 21, 2018



Copyright © Department of Environmental Fluid Mechanics  
All rights reserved.

---

# Abstract

Climate models predict increased Arctic precipitation and subsequent Arctic freshening as a response to increased green house gas concentrations. Eulerian studies have shown that with increased Arctic precipitation AMOC (Atlantic Meridional Overturning Circulation) strength decreases. Decrease in AMOC strength comes with a decreased redistribution of heat from lower to higher latitudes which can have severe effects on our climate. Therefore, understanding the effects and mechanisms of Arctic precipitation change is a crucial building block for predicting and possibly preventing climate change. This study used a Lagrangian approach. The pathways of water at Fram Strait were investigated for present-day climate (control run) and two scenario runs with increased Arctic precipitation (+50% and +300% respectively). Importantly, it was found that Arctic water reaches the Labrador Sea through Denmark Strait for all three runs. Thus, the extra fresh water in the Arctic can possibly impact sinking and convection zones in the Labrador Sea. The total amount of Arctic water, passing Denmark Strait from Fram Strait, increases for the weak scenario and decreases for the strong scenario of this study. On the other side of Iceland, for the strong scenario of this study, Arctic water stops passing the Iceland-Faroe-Ridge through the Faroe Bank Channel. The amount of Arctic water going into and staying in the Nordic Seas remained almost unchanged with increased Arctic precipitation. The two routes passing from Fram Strait into the North Atlantic were analysed further with respect to depth changes and properties. On both routes particles were fresher compared to the control run when increasing Arctic precipitation. For the weak scenario particles were usually colder than the control run on both routes. For the strong scenario, particles were only colder at Fram Strait, but got warmer than the control run along the pathway.



---

# Table of Contents

<b>Acknowledgements</b>	<b>xi</b>
<b>1 Introduction</b>	<b>1</b>
<b>2 Theoretical background</b>	<b>3</b>
2-1 Currents in the Arctic and North Atlantic Ocean . . . . .	3
2-2 Atlantic Meridional Overturning Circulation . . . . .	7
2-3 Possible changes of the overturning circulation in a warming climate . . . . .	9
2-4 Previous research . . . . .	10
2-5 Research questions . . . . .	12
<b>3 Models and model performance</b>	<b>13</b>
3-1 EC-Earth . . . . .	14
3-1-1 Model description . . . . .	14
3-1-2 Model performance and model runs . . . . .	15
3-2 Connectivity Modelling System . . . . .	22
3-2-1 Model description . . . . .	22
<b>4 Lagrangian tracking of Arctic Water into the North Atlantic</b>	<b>25</b>
4-1 Tagging Arctic precipitation . . . . .	25
4-1-1 Tagging Arctic Precipitation - Results . . . . .	26
4-2 Tracing Arctic Waters . . . . .	28
4-2-1 Tagging particles with transport . . . . .	29
4-2-2 Pathway categories . . . . .	30
4-2-3 Analysing properties - temperature salinity . . . . .	31

---

<b>5</b>	<b>Effects of increasing Arctic precipitation on the pathways and properties of the waters in Fram Strait</b>	<b>33</b>
5-1	Pathways of the waters passing Fram Strait . . . . .	33
5-1-1	Denmark Strait - a closer look . . . . .	39
5-2	Properties of the traced water masses . . . . .	41
5-2-1	Properties of the Arctic waters passing Fram Strait . . . . .	41
5-2-2	Changing properties along pathways . . . . .	43
<b>6</b>	<b>Conclusion and Discussion</b>	<b>51</b>
<b>A</b>	<b>CMS</b>	<b>55</b>
A-1	CMS Input files . . . . .	55
A-1-1	Release File . . . . .	55
A-1-2	Run Configuration . . . . .	56
A-1-3	Nest input files . . . . .	57
A-2	CMS Transport tags . . . . .	58
	<b>Bibliography</b>	<b>59</b>
	<b>Acronym</b>	<b>63</b>

---

# List of Figures

2-1	Map of the Nordic Seas and the northern North Atlantic (taken from <a href="https://maps.ngdc.noaa.gov/viewers/bathymetry/">https://maps.ngdc.noaa.gov/viewers/bathymetry/</a> ; names relevant for this section were inserted) . . . . .	4
2-2	Schematic delineation of ocean circulation forming part of the AMOC in the Nordic Seas and subpolar basin (note that deep currents are dashed) <a href="https://www.livescience.com/3883-global-warming-sea-salty.html">https://www.livescience.com/3883-global-warming-sea-salty.html</a> . . . . .	4
2-3	Delineation of the major surface currents in the Arctic and Nordic Seas; deep convection sites are marked dark grey; Acronyms: EGC East Greenland Current, IC Irminger Current, IFF Iceland Faroe Front, JMC Jan Mayen Current, NAC Norwegian Atlantic Current, NIC North Irminger Current (Talley et al., 2011) . . . . .	6
2-4	Delineation of the major surface currents of the North Atlantic; Acronyms: WGC West Greenland Current (Talley et al., 2011) . . . . .	6
2-5	Thermohaline circulation effects illustrated as Ocean Conveyor Belt (from <a href="https://www.nasa.gov/images/content/436189main_atlantic20100325a-full.jpg">https://www.nasa.gov/images/content/436189main_atlantic20100325a-full.jpg</a> ) . . . . .	7
2-6	Example of the AMOC calculated from a model (taken from Katsman (2016)) . . . . .	7
2-7	Deep convection plumes that were simulated in a three dimensional idealised model, plotted over depth and width. Figures show temperature after different time intervals - a,b,c and d showing 2h,12h,24h and 72h respectively. (taken from Olbers et al. (2012)) . . . . .	8
2-8	Illustration of the thermohaline circulation driven by temperature (left) or salinity (right) differences - mechanism is shown over depth and latitude (taken from Katsman (2016)) . . . . .	9
2-9	Analogy for the case of different equilibrium states. Here three equilibrium states are represented by each of the three possible locations of the ball - to get from equilibrium state 1 to 2 and vice versa, a strong 'push' is necessary (taken from Katsman (2016)) . . . . .	9
2-10	Hysteresis diagram of the thermohaline circulation illustrating its equilibria (red and blue line) and the mechanism of abrupt change of northward heat transport (illustrated by the dashed grey and black lines) as a function of the salinity/temperature-forcing ratio. (taken from Katsman (2016)) . . . . .	9

2-11	Maps of the North Atlantic with correlations between the salinity anomaly (dSSS) at grid points vs dSSS at Denmark Strait. The dSSS at the grid points has a lag between $\pm 5$ months and +10 months compared to the dSSS in Denmark Strait (figure taken from van der Sleen (2015)) . . . . .	11
3-1	Flowchart illustrating the flow of information between the models EC-Earth and CMS which were used in this study . . . . .	13
3-2	The tripolar grid ORCA1 (left, taken from Madec (2016)) and the bathymetry of the Arctic and North Atlantic in the ocean model NEMO (right, units = [m]) . . . . .	15
3-3	Representative Concentration Pathways forcing scenarios. Radiative forcing is plotted over time (figure was generated from RCP database accessible at: <a href="https://tntcat.iiasa.ac.at/RcpDb/dsd?Action=htmlpage&amp;page=compare">https://tntcat.iiasa.ac.at/RcpDb/dsd?Action=htmlpage&amp;page=compare</a> ). (Kolb and Riahi, 2009) . . . . .	17
3-4	Mean of the maximum mixed layer depth [m] and mean of sea ice extent (black line) for March of the period 2029-2049 for (a) the control run, (b) scenario wk and (c) scenario str (Katsman et al., 2018) . . . . .	19
3-5	Average of the AMOC transport [Sv] in the basin of the North Atlantic of the final twenty years of simulation (simulations were done 2006-2049), plotted as a function of depth and latitude for (a) the control run and respective anomalies for (b) scenario wk and (c) scenario str (Katsman et al., 2018) . . . . .	20
3-6	Velocities [m/s] and speeds [m/s] at the surface layer (5 m depth) and at 968 m depth in North Atlantic for (a and b) the control run, (c and d) scenario wk and (e and f) scenario str as calculated by EC-Earth . . . . .	21
3-7	Example output of CMS for (a) one particle and n time steps and (b) a zoom in on the first 5 time steps. For these first 5 time steps, the salinity, temperature and depth are indicated as calculated by CMS - note that the first geographical position is the initial seeding location (here at Fram Strait at 30 m depth) for which CMS does not output temperature and salinity . . . . .	22
3-8	Example of 4 <sup>th</sup> order Runge-Kutta method in a 2D velocity field (xtmp1 = temporary x-value 1, ytmp1 = temporary y-value 1, etc) (Paris et al., 2017) . . . . .	23
3-9	Time interpolation pattern for monthly ocean velocity files as implemented in CMS (needs to be used together with the set of equation Eq. (3-3) - also found in Paris et al. (2017)) . . . . .	24
4-1	Pearson's correlation coefficient r between fresh water flux anomaly and salinity anomaly of scenario str relative to the control run for 20 years time series (2006-2026) of (a) Januaries and (b) Junes . . . . .	27
4-2	Average salinity [PSU] (a and c) and fresh water flux anomaly [mm/month] (b and d) for (a and b) January and (c and d) June 2006-2026 between scenario str and control run . . . . .	28
4-3	Seeding location at Fram Strait at 80°N - shown from (a) top view and (b) cross-sectional view. Cross-sectional view shows seeding over depth and longitude - particles coloured blue get advected. . . . .	29
4-4	Pathway categories (Denmark Strait, East Iceland over the Iceland-Faroe-Ridge, Nordic Seas and the Arctic) and their allocation criteria - entering either of the respective orange area(s) as shown in figure. If a particle does not enter any of the outlined areas, it gets allocated to the pathway 'Nordic Seas'. . . . .	31

5-1	Mean transport in (a) absolute quantities [Sv] and (b) relative quantities [%] separated over the different pathways as defined in Figure 4-4 for each of the analysed runs (DenS = Denmark Strait, GrScR = Greenland-Scotland-Ridge, NordicS = Nordic Seas) . . . . .	33
5-2	Horizontal pathways for 20 years advection-time of those particles seeded in Fram Strait in 2027, for (a,d and g) the control run, (b,e and h) scenario wk and (c,f and i) scenario str, which fall into one of the three categories: (a-c) passing Denmark Strait, (d-f) passing east of Iceland over Iceland-Faroe-Ridge or (g-i) staying in the Nordic Seas (note that those particles ending up in the Arctic are not shown since their pathways are less relevant to this study) . . . . .	35
5-3	Particle positions at first time step in the cross section of Fram Strait at 80°N (= seeding location plotted over depth and longitude) color-coded by the pathway they take during 20 years of advection for (a) the control run, (b) scenario wk and (c) scenario str . . . . .	36
5-4	Pathways for 20 years advection-time of those particles seeded in Fram Strait at 80°N in 2027, for (a,d and g) the control run, (b,e and h) scenario wk and (c,f and i) scenario str, which fall into one of the three categories: (a-c) passing Denmark Strait, (d-f) passing over Iceland-Faroe-Ridge or (g-i) staying in the Nordic Seas. Color-coding illustrates the depth [m] along the respective pathway. (Note that this figure is the same as Figure 5-2 with an added colour-coding for depth) . . .	38
5-5	Zoom in on pathways crossing Denmark Strait color-coded according to depth for (a) the control run, (b) scenario wk and (c) scenario str respectively (= zoom in on Figure 5-4 a-c) . . . . .	40
5-6	Particle distribution (a-c) and respective transport distribution [Sv] (d-f) in the cross section of Denmark Strait. Transport is allocated and plotted over depth and longitude based on a grid of 20 m depth by 0.1° longitude. . . . .	41
5-7	Salinity [PSU] (a-c), Temperature [°C] (d-f) and Density [ $kg/m^3$ ] (g-i) of particles seeded in Fram Strait at 80°N over depth and longitude for (a,d and g) the control run, (d,e and f) scenarios 5 and (c,f and i) scenario str. Temperature and Salinity values are taken at first time step of the CMS calculations and the respective density values are calculated. . . . .	42
5-8	Salinity [PSU] (a-c) and Temperature [°C] (d-f) along the horizontal pathways of particles seeded in Fram Strait that pass Denmark Strait for (a and d) the control run, (d and e) scenario wk and (c and f) scenario str . . . . .	44
5-9	Explanatory figure that shows the pathway of one example-particle from Fram Strait to the Labrador Sea passing Denmark Strait (a). The values of three key locations (Fram Strait, Denmark Strait and the most southern tip of Greenland) are highlighted in pink. Plot b shows the properties salinity [PSU], temperature [°C] and depth [m] of the same particle over time. The values at the time when the particle is at the key locations, as shown in plot a, are again highlighted in pink. 45	45
5-10	Mean temperature [°C] of the Arctic waters passing Denmark Strait at three key locations (FramS = Fram Strait, DenS = Denmark Strait, TGreen = southern tip of Greenland) for the control run, scenario wk and scenario str (a). And temperature changes [°C] between the respective key locations for all three runs (b) . . . . .	46
5-11	Mean salinity [PSU] of the Arctic waters passing Denmark Strait at three key locations (FramS = Fram Strait, DenS = Denmark Strait, TGreen = southern tip of Greenland) for the control run, scenario wk and scenario str (a). And salinity changes [PSU] between the respective key locations for all three runs (b) . . . . .	47
5-12	Salinity [PSU] (a and b) and Temperature [°C] (c and d) along the horizontal pathways of particles seeded in Fram Strait that pass Iceland Faroe Ridge for (a and d) the control run and (d and e) scenario wk. . . . .	47

5-13	Explanatory figure that shows the pathway of one example-particle from Fram Strait to the Labrador Sea passing the Faroe Bank Channel (a). The values of three key locations (Fram Strait, Faroe Bank Channel and south of Iceland) are highlighted in pink. Plot b shows the properties salinity [ <i>PSU</i> ], temperature [ $^{\circ}C$ ] and depth [ <i>m</i> ] of the same particle over time. The values at the time when the particle is at the key locations, as shown in plot a, are again highlighted in pink.	48
5-14	Mean temperature [ $^{\circ}C$ ] of the Arctic waters passing on the east of Iceland into the North Atlantic at three key locations (FramS = Fram Strait, FaroeB = Faroe Bank Channel, Slce = south of Iceland) for the control run, scenario wk and scenario str (a). And temperature changes [ $^{\circ}C$ ] between the respective key locations for all three runs (b)	49
5-15	Mean salinity [ <i>PSU</i> ] of the Arctic waters passing on the east of Iceland into the North Atlantic at three key locations (FramS = Fram Strait, FaroeB = Faroe Bank Channel, Slce = south of Iceland) for the control run, scenario wk and scenario str (a). And salinity changes [ <i>PSU</i> ] between the respective key locations for all three runs (b)	50
A-1	Transport [ <i>Sv</i> ] at Fram Strait calculated (a) directly from the EC-Earth velocity file and (b) interpolated from the EC-Earth velocity file to the particle position	58

---

# List of Tables

3-1	Multiplication factor of the Coupler OASIS3 in EC-Earth for precipitation over the Arctic Ocean (north of 70°N) for the control run, scenario wk and scenario str . . . . .	17
4-1	CMS seeding input information summarized . . . . .	29
4-2	CMS Run Configurations summarized . . . . .	30
5-1	Absolute transport traced southward through Fram Strait for each of the analysed runs . . . . .	33



---

# Acknowledgements

I would like to thank my supervisors Dr Caroline A. Katsman, Prof. Julie D. Pietrzak, Ir. Wim Luxemburg and Steffie L. Ypma for all their feedback and support during the process of writing this thesis. I always felt to be in good hands and I always felt that they were available in moments of need.

Special thanks to my "daily" supervisor Dr Caroline A. Katsman for guiding me throughout the past 9 months. Many thanks for joint brainstorming-sessions, plenty of valuable feedback and always being available in moments of "crisis". I always had the feeling to have support and I learned a lot from her which is very much appreciated.

Also many thanks to Steffie L. Ypma for her help and advice, especially concerning technical challenges and feasibility of ideas. Sometimes I had to fall on my own face first before following her input, but (or maybe therefore) the exchange taught me a lot.

Delft, University of Technology  
June 21, 2018

Selina Catherine Klemm



---

# Chapter 1

---

## Introduction

Climate models predict higher precipitation amounts over the Arctic in response to increased green house gas concentrations in the atmosphere (Bintanja and Andry, 2017). If this higher precipitation leads to net-freshening of the Arctic waters, densities in the Arctic change (the lower the salinity the lighter the water). Ocean circulations are driven by wind and density gradients. Especially the deep circulations depend on density gradients between high and low latitudes. Therefore, if extra Arctic precipitation freshens and consequently alters these density gradients, the present-day circulations change. Whether or rather how much, the Arctic will freshen is an on-going scholarly debate. The water constituting Arctic precipitation can have two origins, namely Arctic evaporation or poleward moisture transport in the atmosphere. Only the latter is the cause of Arctic net freshening. Bintanja and Selten (2014) compared climate models of the CMIP5 (Coupled Model Intercomparison Project) on net freshening and found that on average Arctic surface evaporation changes constitute the larger share of the rainfall increase (namely  $56.4\% \pm 13.2\%$  for a scenario with a relative precipitation increase in the Arctic of up to 60%). However, the highest estimates for the share of poleward moisture transport are two-thirds of the extra precipitation, being particularly pronounced in the summer months. Thus, net-freshening is expected to occur. The therewith predicted changing ocean circulations can have severe effects on our climate. The system of circulations in place today redistributes enormous amount of heat from lower to higher latitudes. A decrease of heat redistribution alters long term climate around the globe and can therewith alter habitats for all kind of species. Considering the possible impacts, achieving a better understanding of the unfolding mechanisms of a freshening Arctic is crucial. Therefore, this research aims to further the current knowledge in this respect. In the following, Chapter 2 gives a more thorough theoretical background of the relevant concepts. The knowledge of these concepts is a prerequisite to understand the approach and its underlying motivation. This study builds particularly on the research done by Van der Sleen (2015). Therefore, some of the results found by Van der Sleen (2015) which motivated the approach of this study are summarised and explained. Subsequently, the research questions are listed. Thereafter, Chapter 3 describes the models used. The research approach is outlined in the Chapter 4. Results are shown in the Chapter 5, and Chapter 6 is dedicated to the discussion and conclusions.

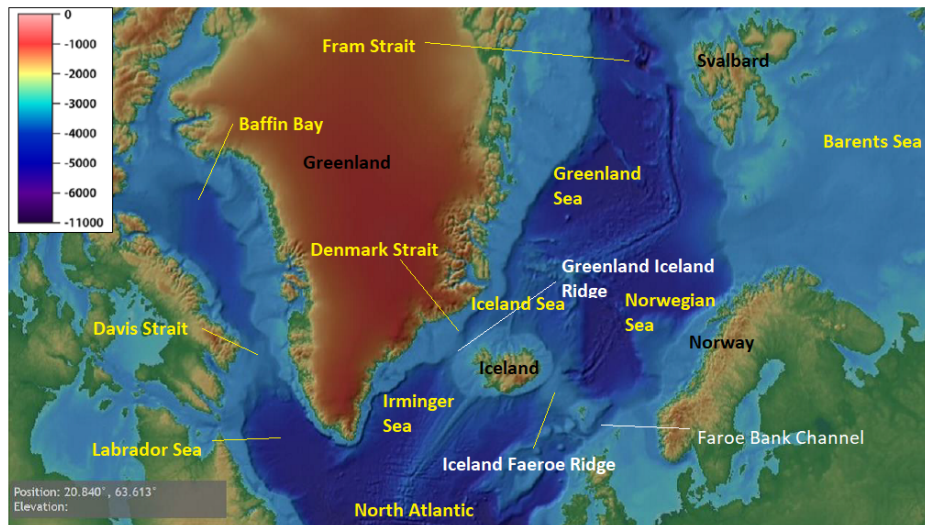


# Theoretical background

The introduction gave a highly simplified overview of the highly complex topic of climate change, the therewith predicted Arctic precipitation change and its effects in the North Atlantic Ocean. This chapter will outline the key concepts relevant to this study in more detail. First, the present state of ocean currents connecting the Arctic with the North Atlantic is described. This description gives a first idea of how water travels in this region and therefore of what we would like to reproduce in the model for a present-day-climate control run. Consecutively, the concept of the Atlantic Meridional Overturning Circulation (AMOC) is explained. This concept is of importance, because it serves as an indicator whether heat is redistributed through ocean currents from lower to higher latitudes. Comparing scenarios to the control run allows looking at changes in strength of the AMOC (and therefore indirectly at changes of heat redistribution). Thereafter, the changing mechanisms of the AMOC, caused by a warming ocean, are outlined. This changing mechanism helps understanding the urgency of gaining further comprehension and insight of global warming and its impact on the ocean. Furthermore, it is an important building stone for understanding how the precipitation change impacts the AMOC. Subsequently, the Eulerian results of Van der Sleen (2015) which motivated the Lagrangian approach of this study are summarised. And finally, the research questions are outlined.

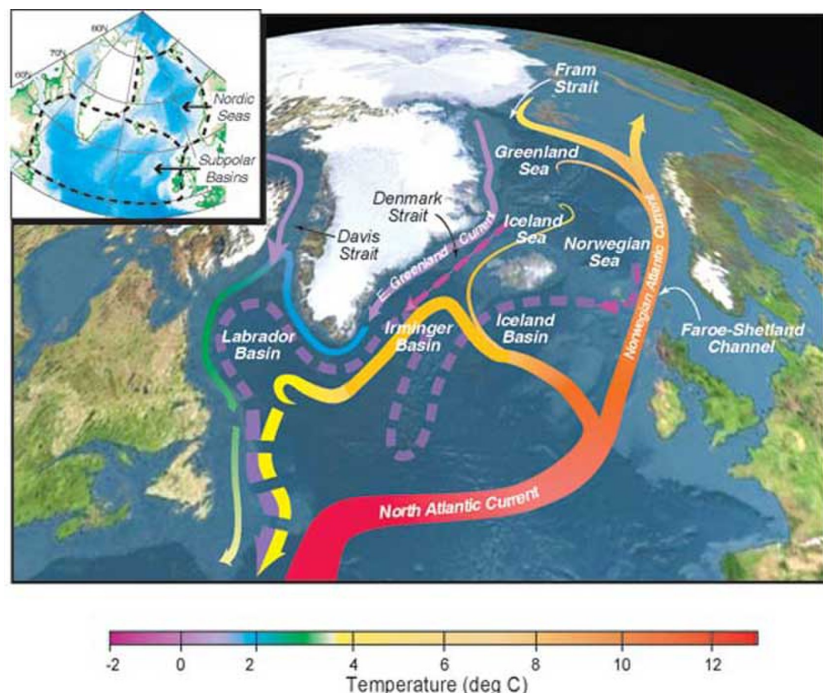
## 2-1 Currents in the Arctic and North Atlantic Ocean

Figure 2-1 shows the region relevant for this study, indicating the geographical landmarks of interest. The Greenland Sea, Iceland Sea and Norwegian Sea are commonly referred to as Nordic Seas or GIN Seas. The Nordic Seas together with the Labrador Sea are of major importance for the ocean mixing, because the most important convection (a process causing vertical mixing of the water column, see Section 2-2 below) and sinking zones are found here. This sinking motion increases the northward transport at the surface of the Atlantic and fuels into transport southward at depth. This also includes a Deep Western Boundary Current (Talley et al., 2011). Consequently, there is an overturning circulation in place. It transports warmer saline waters northward at the surface and fresh



**Figure 2-1:** Map of the Nordic Seas and the northern North Atlantic (taken from <https://maps.ngdc.noaa.gov/viewers/bathymetry/>; names relevant for this section were inserted)

and cold water southward at depth. Figure 2-2 illustrates this phenomenon (warm saline currents are coloured red-orange and deep cold southward currents are coloured purple). Thus, this is a key region for the redistribution of heat from lower to higher latitude. Therefore, the currents of this region are described here in more detail. Note that the currents in the upper layers are mostly wind-driven, while currents at depth are mostly driven by density gradients. The description starts in the Nordic Seas (east towards west) and then goes southward to the North Atlantic (east towards west). At times exceptions are made in order to describe closing circulations or recirculation. Arctic waters may enter the North Atlantic via the southward currents passing the Nordic Seas, most importantly via the East



**Figure 2-2:** Schematic delineation of ocean circulation forming part of the AMOC in the Nordic Seas and subpolar basin (note that deep currents are dashed) <https://www.livescience.com/3883-global-warming-sea-salty.html>

Greenland current. The bulk of Arctic water travelling southward passes Fram Strait (see Figure 2-3). Fram Strait constitutes the deepest connection channel of the Arctic to the world oceans (2600 m). Part of the waters passing the Strait remains in the Nordic Seas, travelling with the Jan Mayen Current (see Figure 2-3). However, most of these waters travel further south passing Denmark Strait either at the surface or at depth (Figure 2-2). In order to pass Denmark Strait the dense waters have to overcome the Greenland-Scotland-Ridge. Therefore, the densest waters stay at depth within the Nordic Seas filling the basins up to crest level (at about 600 m depth) of the ridge (Talley et al., 2011). On the eastern side of Denmark Strait, the North Irminger Current travels northward to then turn east at the northern end of Iceland. This current joins with the warm saline Atlantic water entering the Nordic Seas from the eastern side of Iceland (Figure 2-4). Meanwhile this surface current east of Iceland travels in north-eastern direction, the subsurface current travels the opposite way. This subsurface current is formed by the overflow of the Iceland-Faeroe-Ridge (Perkins and Hopkins, 1998) (dashed purple line in Figure 2-2). On the eastern side of the Nordic Seas, the Norwegian Atlantic Current flows in northern direction. The bulk of this current enters the Arctic through Fram Strait. Parts also deviate into the Barents Sea towards the East and into the East Greenland Current towards the west. The latter subsequently recirculates to the south. East of the Norwegian Atlantic Current exists a separate coastal current which enters into the Barents Sea (see Figure 2-3) (Talley et al., 2011). The net circulation in the Nordic Seas is therefore cyclonic.

South of the Nordic Seas, the East Greenland Current is joined by the Irminger Current and subsequently enters the Labrador Sea to become the West Greenland Current (Figure 2-4). Part of this water keeps travelling north into Baffin Bay and part turns around exiting the Labrador Sea at its southern end as the Labrador Current. The bulk of these waters travels back north and feed the Irminger Current. Thus, the East and West Greenland Current, the Labrador Current and the Irminger Current form a cyclonic circulation known as a subpolar gyre. Between 50°N and 60°N part of the North Atlantic Current turns north along the eastern side of Iceland, part goes north along the western side of Great Britain and part recirculates in the North Atlantic. The first two parts feed the Norwegian Currents within the Nordic Seas. The main contributor to the North Atlantic Current is the Gulf Stream. As becomes apparent, ocean currents form a complex system which operates at different depths. This implies vertical motion of water masses, which leads to the following section describing the Atlantic Meridional Overturning Circulation, short the AMOC.

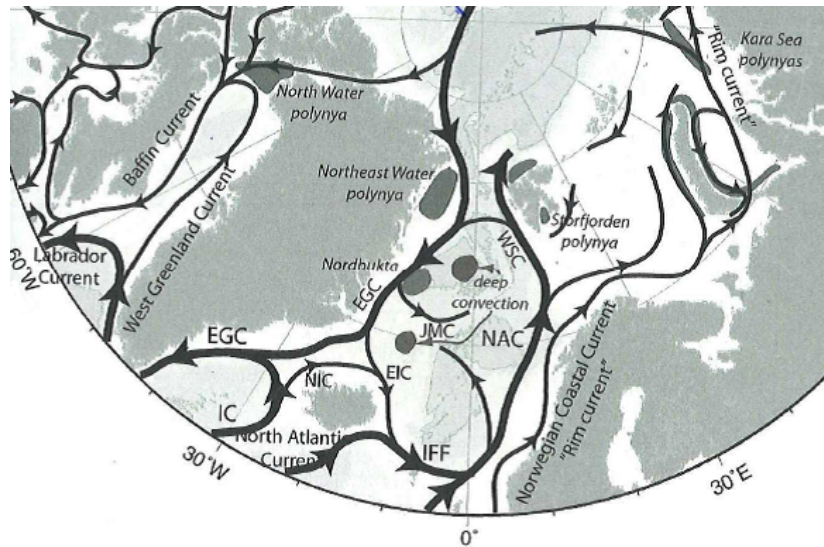


**Figure 2-3:** Delineation of the major surface currents in the Arctic and Nordic Seas; deep convection sites are marked dark grey; Acronyms: EGC East Greenland Current, IC Irminger Current, IFF Iceland Faroe Front, JMC Jan Mayen Current, NAC Norwegian Atlantic Current, NIC North Irminger Current (Talley et al., 2011)

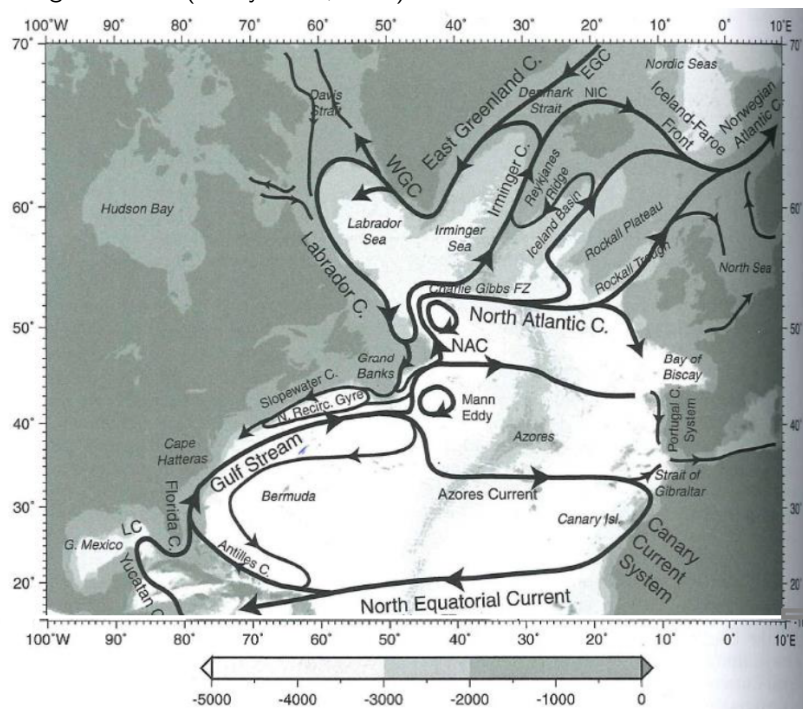


**Figure 2-4:** Delineation of the major surface currents of the North Atlantic; Acronyms: WGC West Greenland Current (Talley et al., 2011)

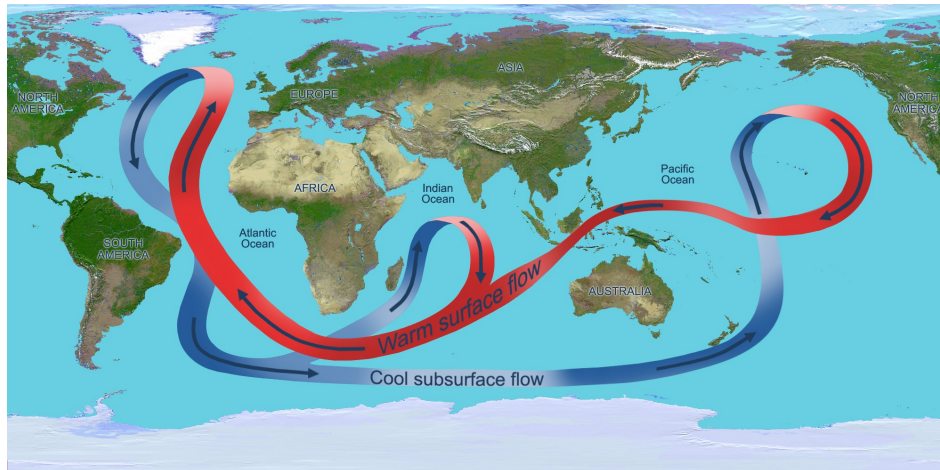


**Figure 2-5:** Thermohaline circulation effects illustrated as Ocean Conveyor Belt (from [https://www.nasa.gov/images/content/436189main\\_atlantic20100325a-full.jpg](https://www.nasa.gov/images/content/436189main_atlantic20100325a-full.jpg))

## 2-2 Atlantic Meridional Overturning Circulation

As mentioned in Section 2-1, there are currents at the surface and currents at depth. This implies that water needs to sink and rise in order to connect the different currents described. This vertical mixing can be quantified with the Atlantic Meridional Overturning Circulation (AMOC). The AMOC describes the meridional (north-south) flow field in latitude-depth plane of the ocean which is driven by wind and density differences. The flow field is integrated in east-west direction, which allows determining volume transports (Rahmstorf, 2007). Figure 2-6 shows an example. Meridional transport is plotted over depth and latitude. It can be seen that in the upper 3000 m the transport is northward, whereas below 3000 m the transport is southward. This results in an overturning motion of the ocean. While the upper ocean circulation is driven primarily by wind stress, the deep ocean circulation is driven by density differences. Water density is primarily determined by its temperature and salinity. Therefore, the density driven mechanism is described by the term thermohaline circulation (THC) (Rahmstorf, 2007), which is often depicted as the Conveyor Belt. Figure 2-5 shows an illustration (note that Figure 2-2 shown in the previous Section 2-1 is a zoom in of this figure). Warm surface flow is depicted in red and cold dense water flowing at depth is coloured blue. Water cools to the point of sinking at high latitudes in the northern Atlantic. The present-day forcing is therefore dominated by temperature (explained further in Section 2-3), but salinity also plays an important role in

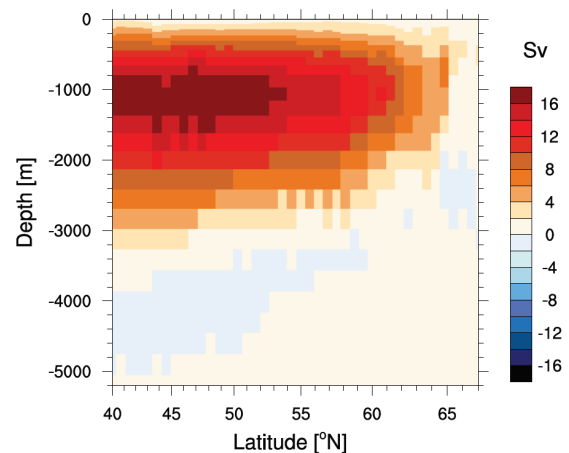


**Figure 2-6:** Example of the AMOC calculated from a model (taken from Katsman (2016))

this temperature-dominated regime. In the North Pacific for example, waters are not saline enough to sink, even when they reach freezing point. Sinking of dense water masses occurs therefore only very locally, where specific conditions are met. On the Northern Hemisphere, sinking occurs in the Greenland Sea and parts of the North Atlantic like the Labrador, the Irminger and the Nordic Seas (for geographical orientation see Figure 2-1). Sinking occurs in the open ocean or at continental slopes. The properties of the waters transported with the AMOC depend considerably on deep convection. Deep convection mixes the water column and determines the properties of deep water which in turn can be entrained by the AMOC. Figure 2-7 visualises the deep convection process. Water gets denser at the surface, due to atmospheric cooling, until it reaches static instability. Then the water column collapses, and forms convection plumes. This mixes the column (potentially even down to the bottom), and it temporarily shows a uniform density. To estimate the depth of deep convection, mixed layer depth can be used.

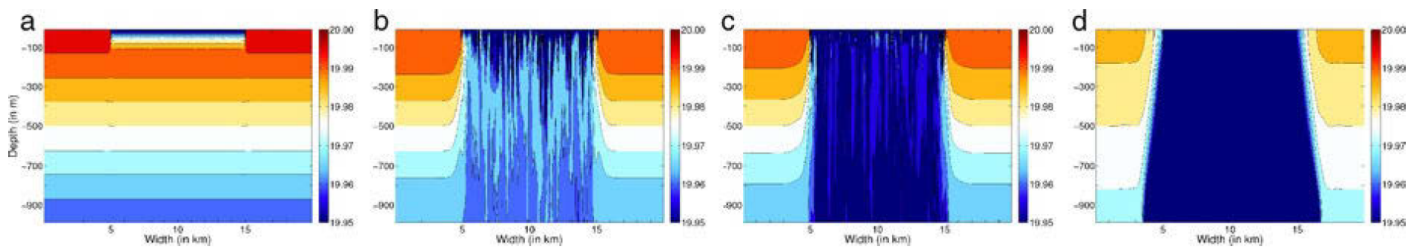


**Figure 2-7:** Deep convection plumes that were simulated in a three dimensional idealised model, plotted over depth and width. Figures show temperature after different time intervals - a,b,c and d showing 2h,12h,24h and 72h respectively. (taken from Olbers et al. (2012))

Mixed layer depth indicates the depth of the water column having the same density. The dense waters formed on top are exchanged with less dense waters from below. Note that this means that deep convection drives the AMOC only indirectly. The properties of the mixed layer, if it is deep enough, determine the properties of the deep currents. (Olbers et al., 2012) If a water body has the lightest water at the surface, and therefore a shallow mixed layer and a stable water column it is called stratified.

So far the ocean circulation system for the northern North Atlantic has been explained, and described more in depth. It was outlined, how the THC together with wind forcing drives the AMOC, and results in a large redistribution of heat from the equator to the higher latitudes. Therefore, the AMOC is an important building stone of our present-day climate. The following section explains possible impacts of a warming climate on this present day state.

## 2-3 Possible changes of the overturning circulation in a warming climate

As mentioned in Section 2-2, the current THC is temperature dominated. It is crucial to know that the effects of temperature differences and salinity differences cause forcing in opposing directions. For a temperature-dominated regime, dense cold waters form at higher latitudes to the point of sinking due to atmospheric cooling. For a salinity-dominated regime, dense saline waters form around the equator due to high evaporation rates as a result of the high incoming solar radiation. A salinity-dominated regime would therefore force water to sink at low latitudes, which means it would force the circulation in the opposite direction. This opposing mechanisms are illustrated in Figure 2-8. The schematics of the overturning of the ocean and its dominating mechanisms are depicted over depth and latitude. For a temperature driven regime, warm low-density water is transported to the poles at the surface and dense cold water returns to the equator at depth. The water absorbs heat at the equator due to solar radiation which is subsequently released back into the atmosphere at higher latitudes. In the case of a salinity dominated regime, saline warm water is transported at depth to the poles and fresher cold water returns from the poles to the equator at the surface. In this regime, the increased salinity at the equator due to evaporation, and the freshening at high latitudes due to increased precipitation, are leading. Thus, multiple equilibria can exist (Stommel, 1961).

Figure 2-9 shows a simplified analogy (Katsman, 2016). The ball can stand still on three different positions, however only two of the positions are stable. Pit #1 would for example stand for a temperature dominated regime, meanwhile pit #2 for a salinity dominated regime. If the ball is pushed hard enough it can travel from one pit to the next.

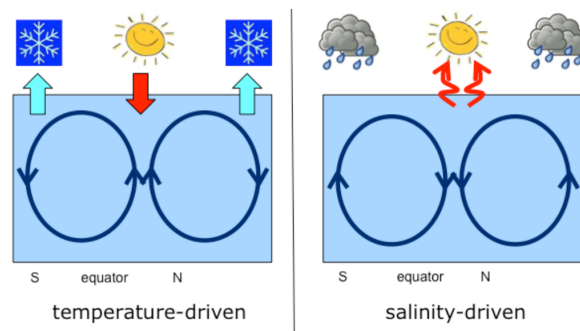


**Figure 2-8:** Illustration of the thermohaline circulation driven by temperature (left) or salinity (right) differences - mechanism is shown over depth and latitude (taken from Katsman (2016))

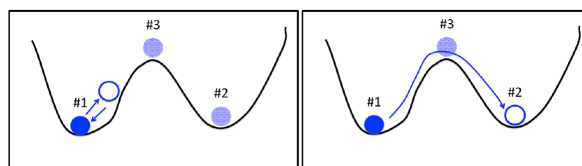


**Figure 2-9:** Analogy for the case of different equilibrium states. Here three equilibrium states are represented by each of the three possible locations of the ball - to get from equilibrium state 1 to 2 and vice versa, a strong 'push' is necessary (taken from Katsman (2016))

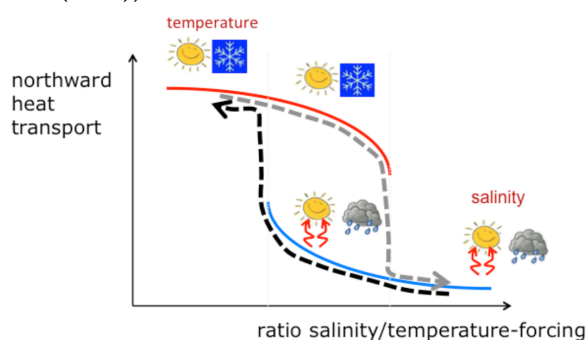


**Figure 2-10:** Hysteresis diagram of the thermohaline circulation illustrating its equilibria (red and blue line) and the mechanism of abrupt change of northward heat transport (illustrated by the dashed grey and black lines) as a function of the salinity/temperature-forcing ratio. (taken from Katsman (2016))

Once a regime is in place it cannot be changed easily. First, the ball would have to be lifted to position #3. In this figurative example, kinetic energy needs to be available to reach the top of the hill. For the AMOC to change equilibrium state, the ratio of salinity-temperature forcing needs to change.

Figure 2-10 illustrates this for the THC in a hysteresis diagram. Northward heat transport is plotted as a function of the ratio of salinity-temperature-forcing. The temperature dominated equilibrium is depicted by the red line, and the salinity dominated equilibrium by the blue line. The dominating driving-mechanism, as already shown in Figure 2-8, is indicated respectively. It should be noted that the heat transport for a temperature dominated regime is much higher than for a salinity dominated regime (Toggweiler and Key, 2003; Katsman, 2016). The present day AMOC is to be found on the red line. As can be seen, the equilibrium changes with a sudden drop of northward heat transport to a salinity domination, once the bifurcation point is overcome (like depicted by the hill (position #3) in Figure 2-9). The bifurcation point is overcome when a certain threshold for the ratio of salinity-temperature forcing is reached. This is illustrated by the end of the red line and the subsequent jump to the blue line, depicted by the dashed grey arrow. This implies a strong sudden decrease in northward heat transport. Crucially, this can only be reversed via the dashed black arrow route. It becomes clear that reversing the effect of a once changed equilibrium would prove difficult. Furthermore, it is important to realise that this jump from one equilibrium to another can cause a very sudden drastic change in our climate and ecosystem (Rahmstorf, 2001; Alley et al., 2003). This is due to the sudden change of northward heat transport. For example, the way nutrients travel in the ocean would completely change, thus altering habitat conditions for many species (Toggweiler and Key, 2003). Furthermore, models predict that the mild European climate would give way to more extreme winters and summers (Jackson et al., 2015; Katsman, 2016).

In present day climate research, it cannot be determined where on the red line our temperature dominated regime is located (Alley et al., 2003). Yet, climate models predict the North Atlantic to freshen and the atmosphere to warm up. The freshening and the decreased atmospheric cooling imply a decreasing density-gradient between the higher and lower latitudes. Therefore, temperature forcing gets weaker and salinity forcing gets stronger. Therefore, the equilibrium state is moving to the right on the grey line (Figure 2-10).

As explained, the impact of increased green house gas concentrations can be severe on the present day ocean circulations, and therefore on the present day climate. The urgency of the issue lies in the possible sudden changes which are difficult to reverse. As explained in Chapter 1, one of the changes, affecting the ratio of temperature-salinity forcing, is the increased Arctic precipitation in response to increased green house gas concentrations. The effects of Arctic precipitation changes is the focus of this study. This study builds on the work done by Van der Sleen (2015), who investigated the effect of Arctic precipitation changes with an Eulerian approach.

## 2-4 Previous research

Van der Sleen (2015) analysed data output from model simulations particularly designed to study the impacts of Arctic precipitation change. Simulations were performed with the coupled climate model EC-Earth (the same model and model runs are also used in this study, and are described further in Section 3-1). He finds that several phenomena change in the

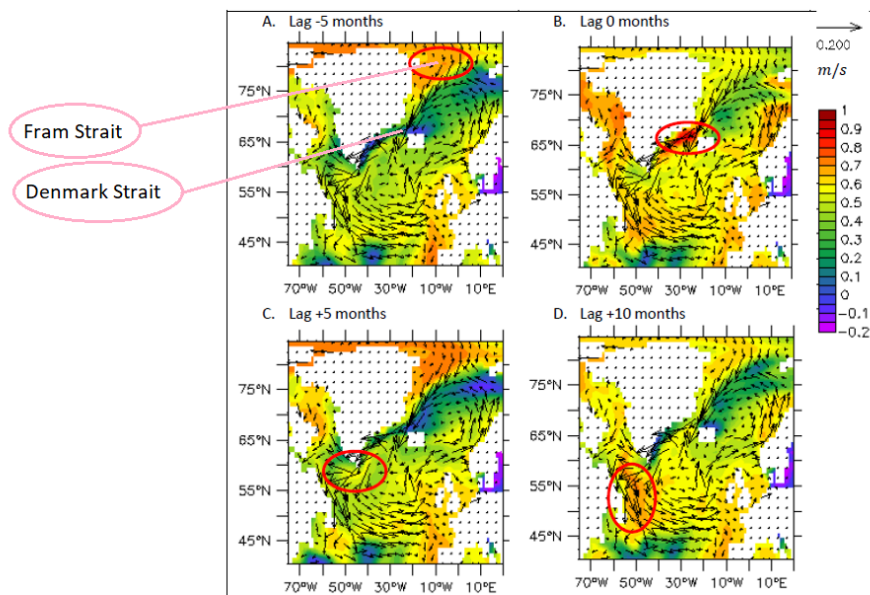


**Figure 2-11:** Maps of the North Atlantic with correlations between the salinity anomaly (dSSS) at grid points vs dSSS at Denmark Strait. The dSSS at the grid points has a lag between  $\pm 5$  months and +10 months compared to the dSSS in Denmark Strait (figure taken from van der Sleen (2015))

North Atlantic, when increasing Arctic precipitation. Local convection zones shift location, or even disappear entirely. Furthermore, the AMOC strength decreases. For a 150% increase of Arctic rainfall compared to the present day climate (control run), this decrease constitutes 43%. However, how this extra fresh water causes these changes, does not become clear in this study. Sleen (2015) hypothesises that extra fresh water is advected to the North Atlantic making the water column more stable, and thus inhibits convection. He tries to assess the path of the fresh water by making time lapse correlation plots of the salinity anomaly (dSSS) (see Figure 2-11). As can be seen in Figure 2-11 A, the method first seems promising, rendering high correlation for a time lag of five months between dSSS of Denmark Strait (Strait between Greenland and Iceland) and dSSS of Fram Strait (Strait between Greenland and Svalbard). However, when looking five months into the future (Figure 2-11 C), it is unclear how the salinity anomaly travels exactly. Hence, the limitations of the Eulerian approach with respect to identifying the pathways of the Arctic freshwater show. Observing a fixed space in time (Eulerian approach) does not allow for observing the changing properties of a specific water mass. Mixing effects are not taken into account and there is no certainty where the Arctic water goes. Thus, it remains unclear where, and therefore how the fresh water impacts the AMOC, the sinking and convection areas. This study tries to further the knowledge with this respect.

## 2-5 Research questions

In order to study where and how the increasing Arctic precipitation impacts the ocean circulations, this research will use a Lagrangian approach. The Lagrangian approach follows a water mass over space and time (contrary to the Eulerian approach, which looks at a fixed location over time). Thus, the pathways of a water volume in the North Atlantic, and therefore possible impact locations, can be clearly identified. Furthermore, it can be observed how a specific water mass changes its properties, such as salinity, temperature and depth over space and time. For this Lagrangian study, the following research questions have been formulated.

1. Can the Arctic precipitation change be clearly identified in the model in order to trace its pathways numerically?
2. What pathways does the Arctic water passing southward through Fram Strait travel and what volume transports do the different pathways carry?
3. How does the above change if the Arctic precipitation increases in the scenarios?
4. How and where do the properties (salinity, temperature) of initially seeded particles change in the scenarios? And how does that differ when comparing it to the control run?
5. More generally, does the Lagrangian approach add value in order to answer the questions above?

In the following, Chapter 3 describes the available model data and models. Thereafter, the research approach is outlined in the Chapter 4. Results are shown in the Chapter 5 and Chapter 6 is dedicated to discussion and conclusions.

# Models and model performance

The following gives a description of the tools and their output used in this research. Figure 3-1 illustrates the flow of information between the different models. This section is structured according to this information-flow. As can be seen, models include the coupled climate model EC-Earth and the numerical modelling system CMS (Connectivity Modelling System). The first section of this chapter is therefore dedicated to EC-Earth. Firstly, the model components and secondly, the output of the model are described. The latter includes the simulation quality of the control run (present-day climate) for the areas relevant to this study and the scenarios with increased precipitation. The oceanographic files of the control run and the scenarios are input for CMS. The second section of this chapter describes the model components of CMS, its additionally required input (release files) and the resulting output.

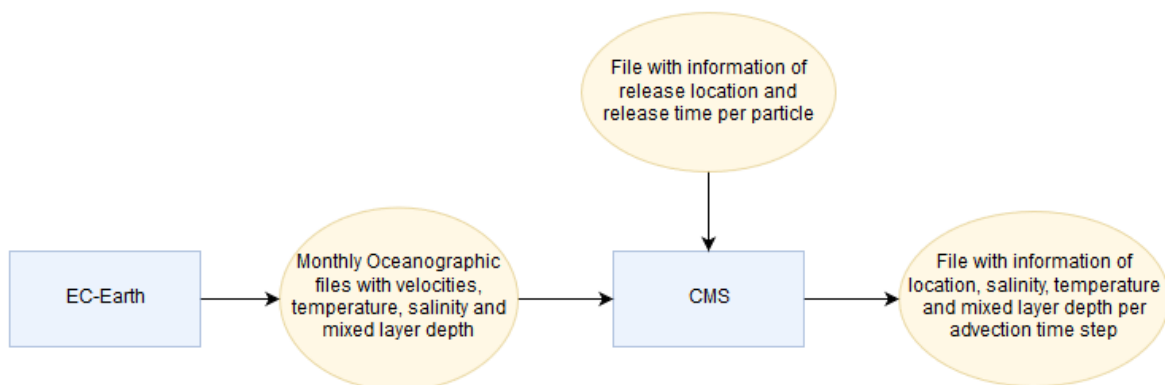


**Figure 3-1:** Flowchart illustrating the flow of information between the models EC-Earth and CMS which were used in this study

## 3-1 EC-Earth

### 3-1-1 Model description

EC-Earth is a coupled earth system model, modelling ocean-atmosphere-sea ice-land interactions. Its main components are the ocean model, Nucleus for European Modelling of the Ocean, short NEMO, and the atmosphere model, Integrated Forecast System, short IFS. NEMO has been developed by the Institute Pierre Simon Laplace (IPSL). In order to include sea ice simulation, the Louvain-la-Neuve Sea Ice model (LIM) made by the University of Louvain-la-Neuve has been integrated into NEMO. The European Centre for Medium Range Weather Forecasts (ECMWF) developed IFS. It includes the Tiled ECMWF Scheme for Surface Exchange over Land (HTESSEL) (Balsamo et al., 2009). The coupler OASIS3 (Ocean, Atmosphere, Sea Ice, Soil, version 3) couples the land/atmosphere model with the ice/ocean model. (Madec, 2016), (Sterl et al., 2012)

NEMO (version 2) is an ocean general circulation model combining Océan Parallélisé version 9 (OPA9) and LIM2. It uses primitive equations and a free surface. A curvilinear C-grid and a z-coordinate are used for the horizontal and vertical discretization respectively (Sterl et al., 2012). NEMO provides for different choices of numerical algorithms and physical parametrization. For EC-Earth momentum advection is chosen to be energy- and enstrophy-conserving. Free slip is used as lateral boundary condition. Harmonic operators are combined with biharmonic operators for horizontal momentum diffusion. A TVD advection scheme is used for the tracer equations. Furthermore, a Laplacian diffusion operator for salinity and temperature is applied. It diffuses isopycnal thickness through an adiabatic mixing scheme. Vertical mixing is calculated by Gaspar's turbulent kinetic energy scheme, where the mixing length depends on the local density profile. These and more choices for the EC-Earth configuration of NEMO can be found here: <http://eearth.knmi.nl/index.php?n=PmWiki.Pre-IndustrialControlRun>. Furthermore, EC-Earth uses the ORCA1 configuration which implies a resolution of  $1^\circ \times 1^\circ$ . The grid is refined towards the equator to  $1/3^\circ$ . Since the North Pole is not placed on land like its Southern equivalent, its discontinuity is avoided with a tripolar grid. Therefore, coordinate poles are placed on land in Canada and Siberia (see Figure 3-2). Figure 3-2 also shows the model bathymetry for the Arctic and the North Atlantic. NEMO consists of 42 layers which increase in thickness with depth. In the upper 100-300 m, layers are around 10 m thick, and the bottom layer, at about 5,500 m depth, reaches 300 m thickness. (Hazeleger et al., 2012) (Madec, 2016) (Sterl et al., 2012)

The sea ice model LIM 2 uses the same grid as NEMO. Sea ice is modelled as a 2 dimensional layer that acts as stress-communicator between atmosphere and ocean. The model simulates the thermodynamic processes of the sea ice by considering a snow sheet on top of the sea ice cover. LIM is described in detail by Fichefet and Marquedda (1997). More information about the atmosphere model IFS (version 31r1) can be found in Hazeleger et al. (2012) and at <https://www.ecmwf.int/>.

The coupler OASIS3 operates with a couple frequency of every 3 hours. Then IFS/HTESSEL receives sea surface temperature, surface ocean velocity, sea ice fraction, sea ice temperature and snow thickness over sea ice from NEMO/LIM. And NEMO/LIM is provided with surface heat flux, snowfall, freshwater flux and wind stress by IFS/HTESSEL (Hazeleger et al., 2012). For more information on the coupler OASIS3, see the user guide at [http://www.cerfacs.fr/oa4web/papers\\_oasis/oasis3\\_UserGuide.pdf](http://www.cerfacs.fr/oa4web/papers_oasis/oasis3_UserGuide.pdf) (Valcke, 2006).

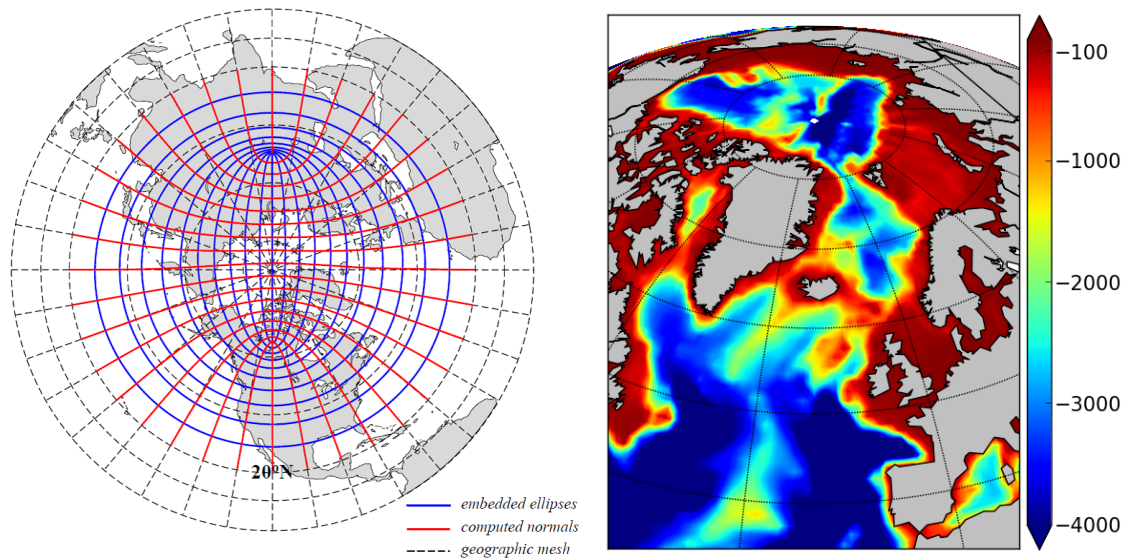


**Figure 3-2:** The tripolar grid ORCA1 (left, taken from Madec (2016)) and the bathymetry of the Arctic and North Atlantic in the ocean model NEMO (right, units = [m])

### 3-1-2 Model performance and model runs

This section outlines the three different model runs which are studied. Firstly, the control run representing the present day climate is scrutinized with respect to its simulation quality, and secondly, some of the changes in the two scenario runs with increased precipitation are shown.

#### Simulation Quality of the control run

The journal *Climate Dynamics* publishes in its Volume 39, Issue 11 articles dealing with the performance and results of EC-Earth. Sterl et al. (2012) focus on the performance of the ocean component in the coupled model in comparison to current observations. They find that the mean state, meaning the mean temperature, salinity, ocean circulation and sea ice, is generally reproduced well. However, the state-of-the-art climate models do not allow an exact reproduction of reality. Thus, temperatures between the equator and  $40^{\circ}N/S$  are too cold, and above  $40^{\circ}N/S$  too warm. Furthermore, the surface waters show generally too low salinities.

The large circulations are successfully simulated. For the North Atlantic the subtropical gyre circulation with westward intensification, namely the Gulf Stream, is captured. The current, known as the Gulf Stream is not narrow enough and is not located in the correct position. Yet, this is a short-coming observed in all coarse ocean models due to high viscosity-values. In order to maintain numerical stability, viscosity in these models is set unreasonably high. Vitally for this study, the subpolar and polar gyres are found south of Greenland and in the Nordic Seas respectively. The subpolar gyre extends not far enough to the south.

In the Arctic, sea ice extent is reproduced well, though its thickness is overestimated. Sea ice transport through Fram Strait is in variability and on average well reproduced. This is important, since the amount of sea ice reaching the Labrador Sea plays a major role in reducing

deep convection. This could be affecting the AMOC strength. AMOC variation influences in turn air temperature in the North Atlantic which affects sea ice. (Sterl et al., 2012)

The overturning circulation relevant for this study, the AMOC, shows a result which is generally low compared to observations (Sterl et al., 2012): 14.5 Sv<sup>1</sup> in the model vs 18.7 Sv in observations (Kanzow et al., 2010). Furthermore, the maximum of the overturning is found at 800 m, which is too shallow compared to observations (1100 m (Kanzow et al., 2010)). Yet, its heat transport is captured well (Sterl et al., 2012).

Overall, EC-Earth is a state-of-the-art climate model as is widely used in climate research. Though not able to capture all the details as outlined in Section 2-1, EC-Earth does reproduce the main characteristics of the ocean circulation. In order to study the effect of Arctic precipitation change, a series of runs were performed. The following section describes the scenario runs which were done to investigate the impact of increased Arctic precipitation in the North Atlantic.

### EC-Earth Scenario Runs with increased Arctic precipitation

In this research, the effect of increased Arctic precipitation is studied. A control run simulates the present-day climate and two scenario runs, with an extra fresh water input over the Arctic Ocean, simulate the effect of increased precipitation. Other climate change traits like for example atmospheric temperature, only change as a feedback response of this increased precipitation. The extra precipitation "simply appears" in the model, which means the water balance is not closed. This is done by adding a multiplication factor to the coupler OASIS3 (Eq. (3-1)). Thus, the precipitation amount north of 70°N calculated by IFS is multiplied in OASIS3 before being transferred to NEMO. This approach allows to isolate the effects of extra Arctic precipitation from other climate change phenomena.

$$Precipitation_{latitude > 70^{\circ}N, OASIS3} = \gamma * Precipitation_{latitude > 70^{\circ}N, IFS} \quad (3-1)$$

$\gamma$  = multiplication factor

$Precipitation_{IFS}$  = precipitation as calculated by IFS

$Precipitation_{OASIS3}$  = increased precipitation according to chosen climate scenario

A series of runs with different  $\gamma$ -values has been performed, meaning runs with different precipitation increase. Due to the limited scope of this study, only two scenario runs are used. The two scenarios chosen are labelled 'weak' and 'strong'. The weak scenario will be referred to as scenario wk, and the strong scenario will be referred to as scenario str. The scenario str is characterised by a  $\gamma$ -value of 4, and therefore constitutes a rather unrealistically strong scenario. It was done in order to produce a strong signal, and thus show the impact of increased Arctic precipitation very clearly. Scenario wk uses a  $\gamma$ -value of 1.5. This is based on the estimated increase of Arctic precipitation for the Representative Concentration Pathways (RCP) Scenario 8.5. The RCP-Scenarios, are four different future scenarios of radiative forcing levels in 2100 (see Figure 3-3). Radiative forcing is determined by emissions, concentrations and land-cover change projections (Kolb and Riahi, 2009). The RCP scenarios are widely used in climate research and make different studies comparable. A summary of the scenarios used in this study can be found in Table 3-1.

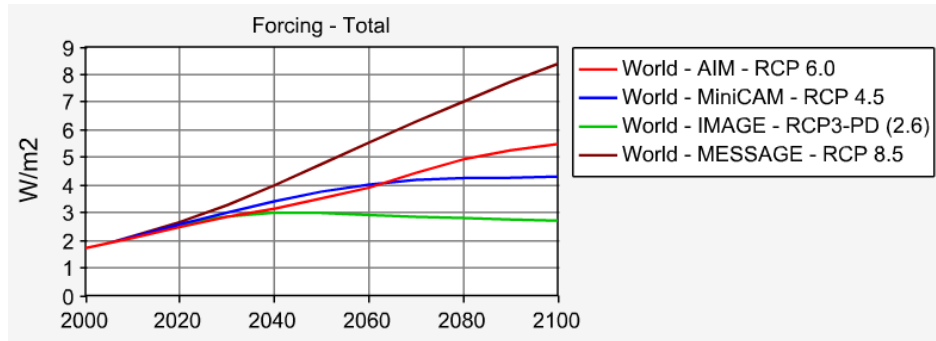


**Figure 3-3:** Representative Concentration Pathways forcing scenarios. Radiative forcing is plotted over time (figure was generated from RCP database accessible at: <https://tntcat.iiasa.ac.at/RcpDb/dsd?Action=htmlpage&page=compare>). (Kolb and Riahi, 2009)

Run	$\gamma$ -value	type
control run	1	-
scenario wk	1.5	RCP 8.5
scenario str	4	for strong effect

**Table 3-1:** Multiplication factor of the Coupler OASIS3 in EC-Earth for precipitation over the Arctic Ocean (north of 70°N) for the control run, scenario wk and scenario str

The control run and the scenario runs are modelled for a period of 45 years (2006-2049). The mixed layer depth and the AMOC strength decrease with increasing Arctic precipitation. The reduction of the mean mixed layer depth of a period of 20 years for the month of March can be seen in Figure 3-4. As expected, the effect is a lot less pronounced in the weakly forced scenario (Figure 3-4 b) than in the strongly forced scenario (Figure 3-4 c). Figure 3-4 also shows the sea ice edge (black line). The change of this edge seems to be minor for scenario wk. In the strong scenario, the deepest areas of mixed layer depth entirely disappear and only shallow mixed layer west of Norway and south of Iceland remains. The sea ice extent increases drastically in the Labrador Sea and beyond. Bintanja et al. (2018) also find that artificially increased precipitation increases sea ice expansion and trigger atmospheric cooling near the surface. They show that this is due to a decrease in upward ocean heat flux which is the result of increased stratification caused by the extra fresh water input.

The AMOC strength of the control run and the AMOC strength anomalies for the scenarios can be seen in Figure 3-5 a-c. The AMOC strength decreases by up to 2 Sv and up to 7 Sv for scenario wk and scenario str, respectively. Considering that the AMOC strength of the control run reaches values up to 18 Sv, these are considerable changes.

Figure 3-6 shows the horizontal velocities and speeds at the surface layer (5 m depth), and at 968 m depth in North Atlantic for Figure 3-6 a and b the control run, Figure 3-6 c and d scenario wk and Figure 3-6 e and f scenario str as calculated by EC-Earth.

At the surface layer (Figure 3-6 a, c and e) the cyclonic circulation within the Nordic Seas, as described in Section 2-1, is reproduced. It can be seen that this circulation strengthens with increasing Arctic precipitation. On the western side of the Nordic Seas, the East Greenland current is clearly modelled. It narrows and increases strength with increasing Arctic precip-

<sup>1</sup>Sv = Sverdrup =  $10^6 \frac{m^3}{s}$

itation. This current transports Arctic water into the North Atlantic and the Labrador Sea which means it is of special interest to this study. Furthermore, the subpolar gyre of the Labrador and Irminger Sea is visible, as is the North Atlantic current flowing northward into the Nordic Seas (compare with Figure 2-3 and Figure 2-4). While changes of the subpolar gyre do not become clearly apparent in this figure, the North Atlantic current slightly weakens at the surface layer. At 968 m depth (Figure 3-6 b, d and f) the subpolar gyre weakens more visibly with increasing Arctic precipitation, and the circulation of the Nordic Seas changes entirely in shape and directions. Furthermore, the velocities at Denmark Strait and the Faroe Bank Channel decrease.

While these changes help making assumptions about what will happen to the waters in Fram Strait with increasing Arctic precipitation, they do not give accurate knowledge of the pathways. It should be kept in mind that the model has 42 layers over depth, and also vertical velocities which are not shown here.

The output of these model runs, oceanographic data files, constitute the input for the Lagrangian analysis (Chapter 4 onwards). The oceanographic data files used contain monthly values of the 3D ocean velocities, temperature, salinity and mixed layer depth. The Lagrangian analysis is done with the Connectivity Modelling System, short CMS (described below in Section 3-2).

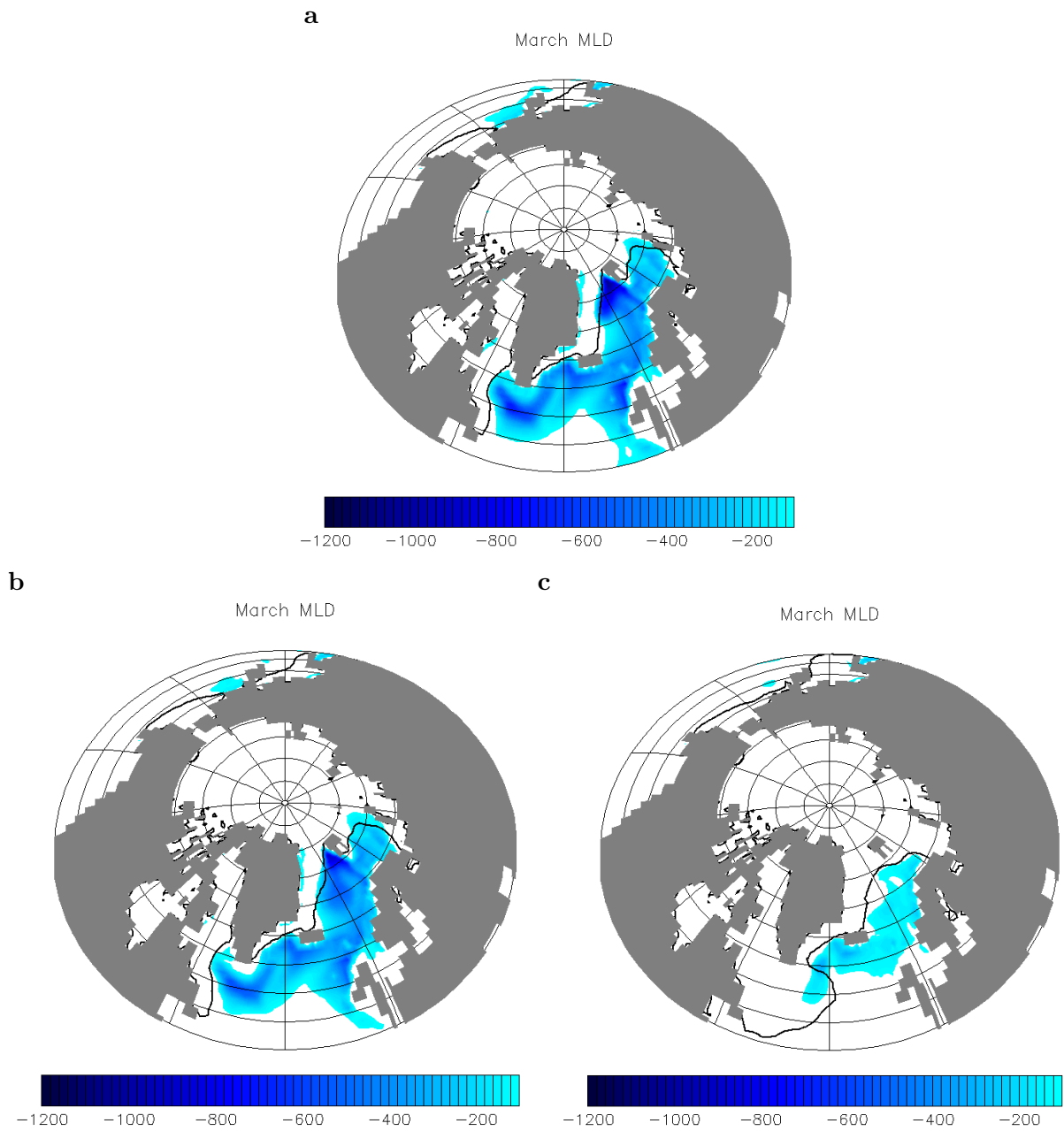


**Figure 3-4:** Mean of the maximum mixed layer depth [m] and mean of sea ice extent (black line) for March of the period 2029-2049 for (a) the control run, (b) scenario wk and (c) scenario str (Katsman et al., 2018)

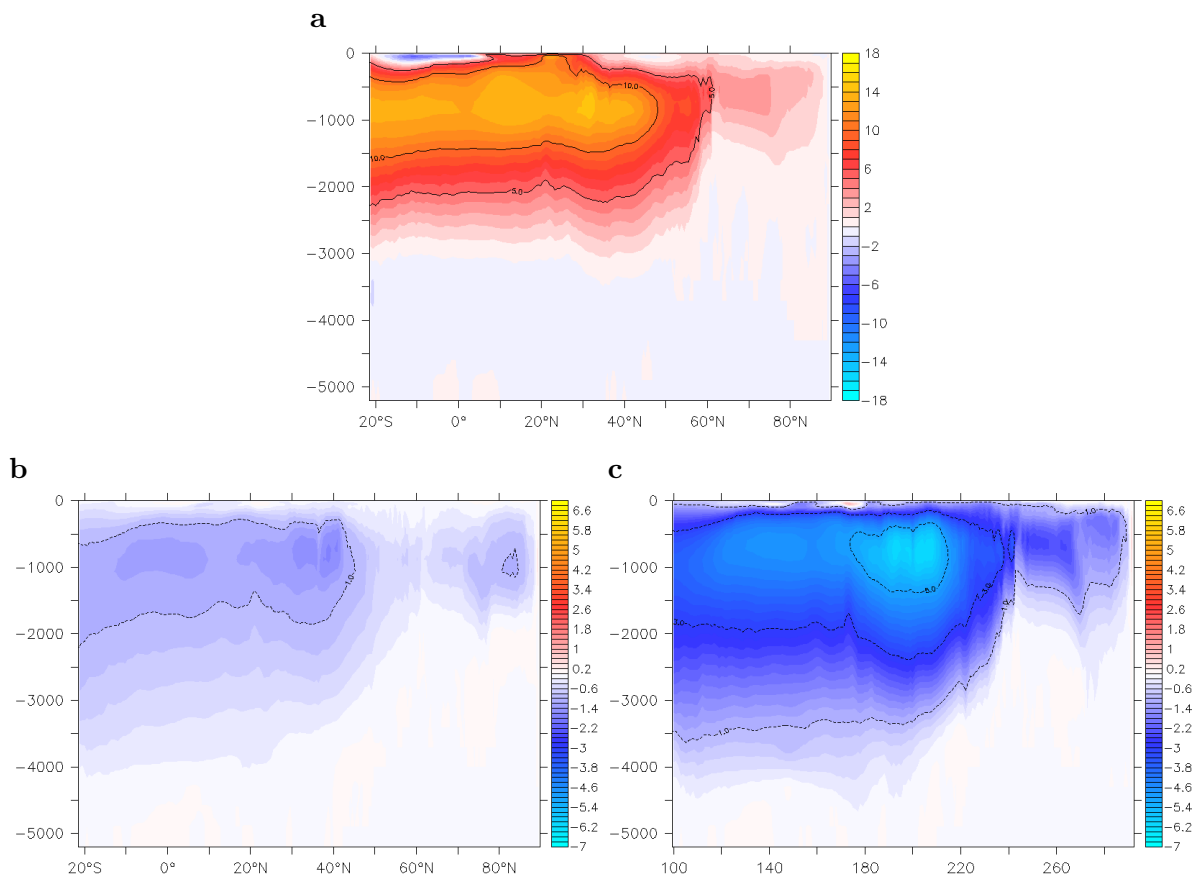


**Figure 3-5:** Average of the AMOC transport [Sv] in the basin of the North Atlantic of the final twenty years of simulation (simulations were done 2006-2049), plotted as a function of depth and latitude for (a) the control run and respective anomalies for (b) scenario wk and (c) scenario str (Katsman et al., 2018)

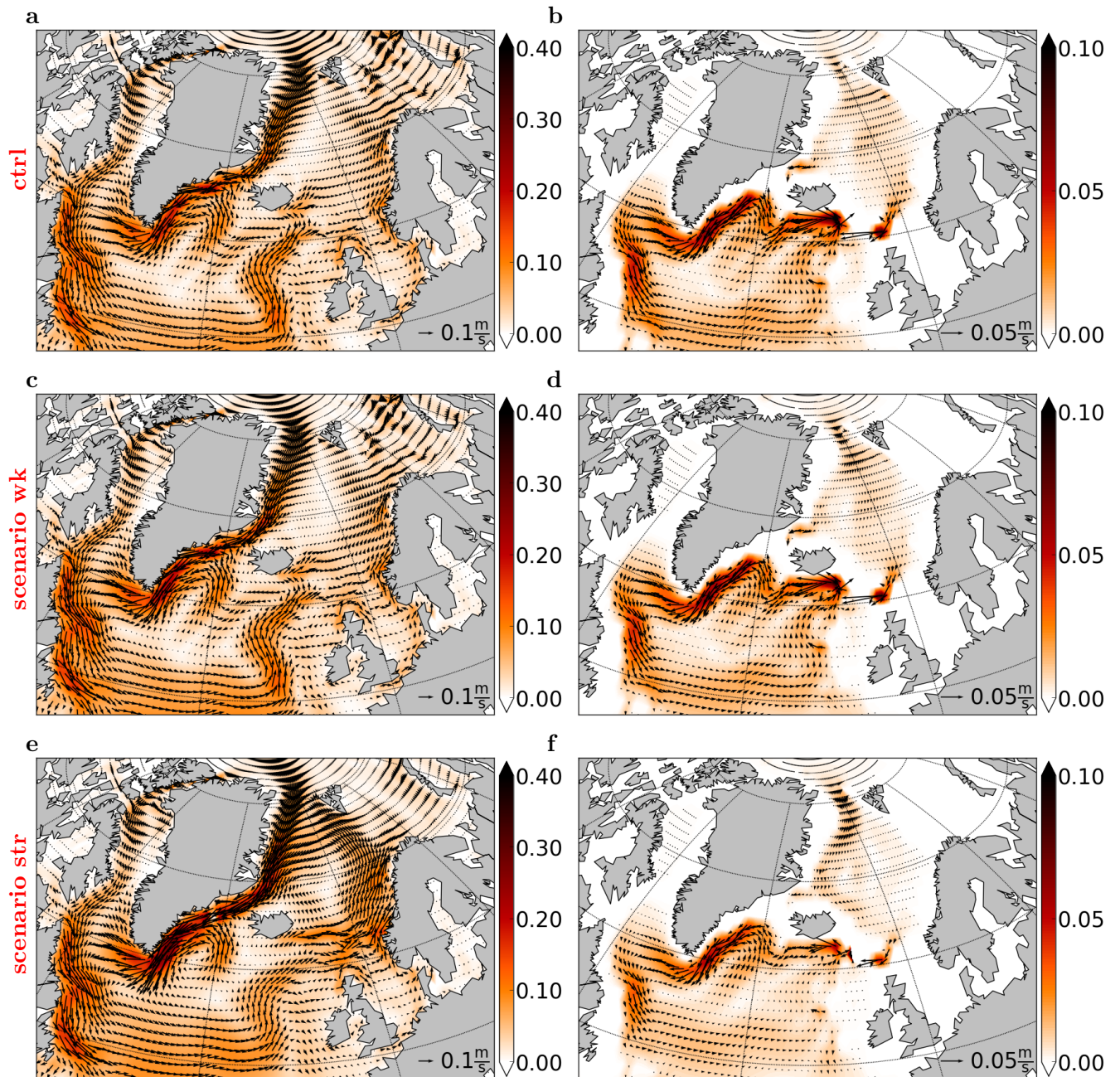


**Figure 3-6:** Velocities [m/s] and speeds [m/s] at the surface layer (5 m depth) and at 968 m depth in North Atlantic for (a and b) the control run, (c and d) scenario wk and (e and f) scenario str as calculated by EC-Earth

## 3-2 Connectivity Modelling System

In order to perform the Lagrangian analysis of the velocity fields produced with EC-Earth, the Connectivity Modelling System (CMS) is used. CMS is an open source, biophysical modelling system which uses a stochastic Lagrangian framework (Paris et al., 2017). This section describes the set-up and working method of CMS.

### 3-2-1 Model description

CMS can be used to study physical oceanographic phenomena like in this case advection. CMS needs to be given information of where, when and how many particles are to be released and then it uses hydrodynamic fields provided in order to determine individual pathways. A particle represents a small water volume. The smaller the distance between the seeded particles, the smaller the volume of water represented per particle. Furthermore, the respective properties are interpolated to the geographical position at each time step. Properties include salinity and temperature at each location and time step. The location is indicated by latitude, longitude and depth. An example to illustrate the idea is shown in Figure 3-7.

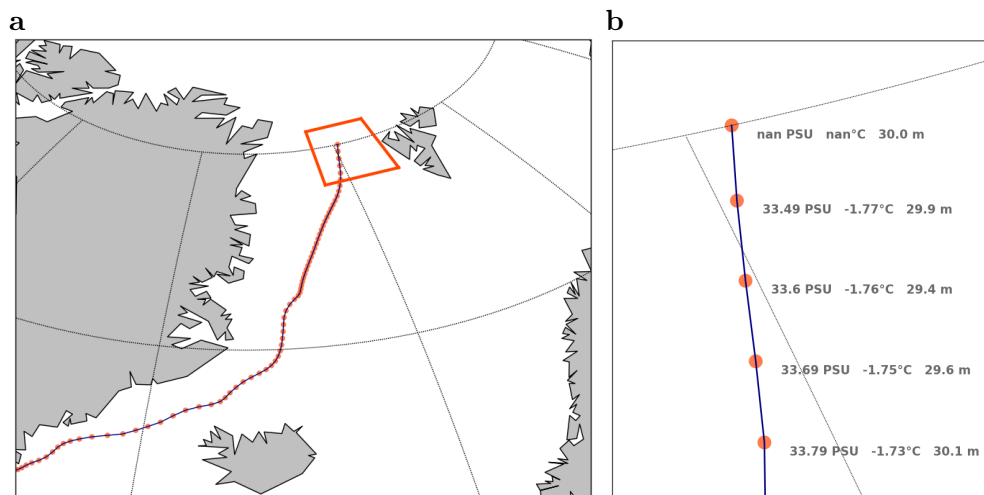


**Figure 3-7:** Example output of CMS for (a) one particle and  $n$  time steps and (b) a zoom in on the first 5 time steps. For these first 5 time steps, the salinity, temperature and depth are indicated as calculated by CMS - note that the first geographical position is the initial seeding location (here at Fram Strait at 30 m depth) for which CMS does not output temperature and salinity

### Building Stones

CMS is built out of several modules. Only the relevant modules are mentioned. The Parallel Module allows for parallel simulations of millions of particles. In this study a couple of hundred of thousands particles are traced per model run. A Landmask Boundary Module makes CMS suitable to track particles over complex ocean topography. Vertical particle movement is flexible through the Vertical Movement Module, which allows to simulate sinking and rising of par-

ticles. This module includes among others buoyancy, upwelling and subduction. (Paris et al., 2017)

### Integration Method

The weighted average of velocities at different time steps is used to calculate particle advection. In CMS this is done with a 4<sup>th</sup> order Runge-Kutta scheme in order to improve accuracy compared to a simple extrapolation. For each Runge-Kutta step, three (3D) times four local velocities are required to calculate the new particle position. One set of velocities (u,v,w) is obtained from the old particle position, and three sets of velocities (3 times (u,v,w)) are obtained from new particle position. The new positions are calculated twice after half a time step, and once after a whole time step.

An example for a 2D velocity field can be seen in Figure 3-8. Next these velocities are used to calculate the final velocities  $u_f, v_f, w_f$  and consequently, the new position  $x_{new}, y_{new}, z_{new}$  at time  $t + timestep$ . This procedure is expressed by the set of Eq. (3-2).

$$\begin{aligned}
 u_f &= (u_1 + 2 * u_2 + 2 * u_3 + u_4) \\
 v_f &= (v_1 + 2 * v_2 + 2 * v_3 + v_4) \\
 w_f &= (w_1 + 2 * w_2 + 2 * w_3 + w_4) \\
 \Rightarrow (x_{new}, y_{new}, z_{new}) &= (u_f, v_f, w_f) * timestep
 \end{aligned}
 \tag{3-2}$$

$u_1, v_1, w_1 =$  velocities from old position  $x_{old}, y_{old}, z_{old}$  at time  $t$

$u_2, v_2, w_2 =$  velocities at position  $x_{try1}, y_{try1}, z_{try1}$  calculated from  $x_{old}, y_{old}, z_{old}$  with the velocities  $u_1, v_1, w_1$  at time  $t + 0.5 * timestep$

$u_3, v_3, w_3 =$  velocities at position  $x_{try2}, y_{try2}, z_{try2}$  calculated from  $x_{old}, y_{old}, z_{old}$  with the velocities  $u_2, v_2, w_2$  at time  $t + 0.5 * timestep$

$u_4, v_4, w_4 =$  velocities at position  $x_{try3}, y_{try3}, z_{try3}$  calculated from  $x_{old}, y_{old}, z_{old}$  with the velocities  $u_3, v_3, w_3$  at time  $t + timestep$

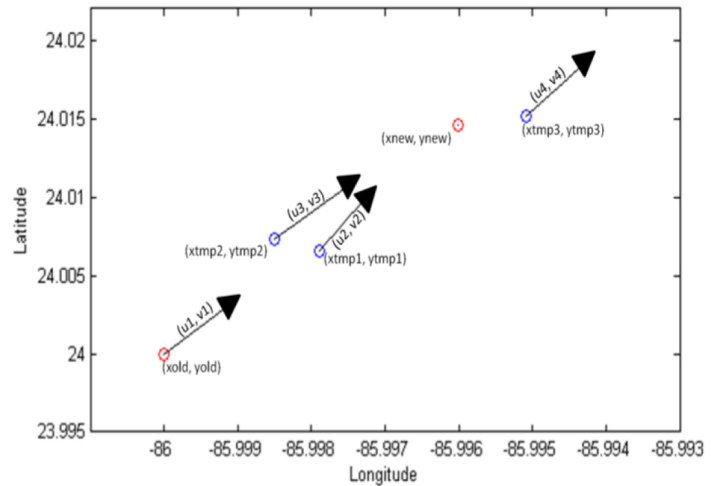


**Figure 3-8:** Example of 4<sup>th</sup> order Runge-Kutta method in a 2D velocity field (xtmp1 = temporary x-value 1, ytmp1 = temporary y-value 1, etc) (Paris et al., 2017)

### Interpolation in space and time

Interpolation in space becomes necessary when a particle's position is not on a grid point (which is nearly always the case). In CMS, two cases of particle position are distinguished. Firstly, a particle may be located such that 64 neighbouring points are located in the ocean, or secondly, a particle may be positioned such that at least one of the 64 neighbouring point is located on land. In the first case, a tricubic interpolation method is used, while in the second case, a trilinear interpolation method is applied. Interpolation in time is required if the time step used for integration is smaller than the time resolution of the oceanographic velocity files. This is the case for this study (more detail about this can be found in the following Chapter 4). For monthly ocean velocity files, as are used here, four files are part of the interpolation. The velocities of the files are weighted according to how close in time a file is to the momentary time step. This is illustrated on an example below with Eq. (3-3) and Figure 3-9).

$$u = (-0.5 * a * b * b * u_1) + (b * (1 + a * (1 - 1.5 * a)) * u_2) + (a * (1 + b * (1 - 1.5 * b)) * u_3) + (-0.5 * b * a * a * u_4) \quad (3-3)$$

$a = 20/31$  (fraction of days advected since last velocity file stored)

$b = 11/31$  (fraction of days to advect until next velocity file stored)

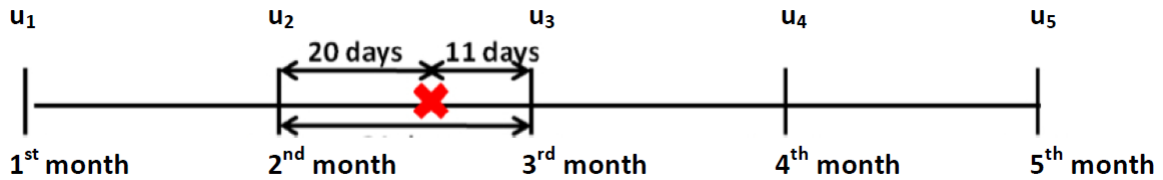


**Figure 3-9:** Time interpolation pattern for monthly ocean velocity files as implemented in CMS (needs to be used together with the set of equation Eq. (3-3) - also found in Paris et al. (2017))

The CMS manual outlining the above and more details can be found here <https://github.com/beatrixparis/connectivity-modeling-system/blob/master/User-Guide-v2.pdf>. The different input parameters and input files which form part of the approach taken specifically in this study are outlined in the Methodology Chapter (Chapter 4). As already mentioned, these input files contain the information of where and when a particle starts to be advected.

This Chapter described the different tools used in this research. Figure 3-1 shows the overall flow of information in the modelling process described in this chapter. The following will outline the approach taken in order to answer the research questions outlined in Section 2-5.

# Lagrangian tracking of Arctic Water into the North Atlantic

The following chapter outlines the approaches taken in order to answer the previously (Section 2-5) defined research questions repeated below. This includes the failed attempt to identify the extra precipitation in the Arctic, and the alternative approach of tracing waters of Fram Strait.

1. Can the Arctic precipitation change be clearly identified in the model in order to trace its pathways numerically?
2. What pathways does the Arctic water passing southward through Fram Strait travel and what volume transports do the different pathways carry?
3. How does the above change if the Arctic precipitation increases in the scenarios?
4. How and where do the properties (salinity, temperature) of initially seeded particles change in the scenarios? And how does that differ when comparing it to the control run?
5. More generally, does the Lagrangian approach add value in order to answer the questions above?

### 4-1 Tagging Arctic precipitation

In order to trace increased Arctic precipitation and determine its pathways with CMS, particles need to be 'seeded' in CMS within the extra Arctic fresh water input only. To identify this fresh water input in the oceanographic output files of EC-Earth, the fresh water fluxes and salinity files were analysed. As described in Section 3-1-2, the precipitation over the Arctic was increased for the scenarios via a multiplication factor in the coupler. Therefore,

it was expected that a fresh water flux anomaly, and thus a salinity anomaly at the surface would be observed in the Arctic when comparing the control run to a scenario run. It was assumed that if a correlation between the fresh water flux anomaly and the salinity anomaly would be found that the water volume with the salinity anomaly at the surface would be extra precipitation. This correlation, measured with the Pearson product moment correlation coefficient  $r$  (Eq. (4-1)), was calculated for a time series of 20 years (2006-2026).

$$r_{\Delta S, \Delta FF} = \frac{cov(\Delta S, \Delta FF)}{\sigma_{\Delta S} * \sigma_{\Delta FF}} = \frac{\sum_{t=1}^n (\Delta S_t - \overline{\Delta S}) * (\Delta FF_t - \overline{\Delta FF})}{\sqrt{\sum_{t=1}^n (\Delta S_t - \overline{\Delta S})^2} * \sqrt{\sum_{t=1}^n (\Delta FF_t - \overline{\Delta FF})^2}} \quad (4-1)$$

$$\begin{aligned} \Delta S(time, lat, lon) &= S(time, lat, lon)_{scen} - S(time, lat, lon)_{ctrl} \\ \Delta FF(time, lat, lon) &= FF(time, lat, lon)_{scen} - FF(time, lat, lon)_{ctrl} \end{aligned}$$

- $S$  = salinity in the Arctic
- $FF$  = vertical fresh water flux (= exchange ocean – atmosphere, negative if net – transport into the ocean)
- $scen$  = scenario run
- $ctrl$  = control run
- $t$  = time step in month
- $n$  = total number of time steps (here 12 months/year \* 20 years = 240 months)

#### 4-1-1 Tagging Arctic Precipitation - Results

Figure 4-1 a and b show Pearson's correlation coefficient  $r_{\Delta S, \Delta FF}$  for scenario str in relation to the control run for January and June, respectively. As can be seen in the plot for January (Figure 4-1 a), the expected positive correlation did not become apparent. In fact, most areas in the Arctic show a negative correlation. This is the case for the majority of the year, except for the summer months June and July. Figure 4-1 b, exhibiting the month of June, shows the expected correlation at least for the European side of the Arctic.

The explanation for this result could be found when looking at the salinity and flux anomalies separately. The twenty year averages of the respective anomalies are shown in Figures 4-2 a and b for January, and in Figures 4-2 c and d for June. While the salinity anomaly figures show very similar plots for the two months, the flux figures show clear differences. For the month of January, the extra fresh water flux entering the Arctic is limited to an area South of Svalbard instead of covering the entire Arctic. Similar results were found for all other months, except for the summer months June, July and August. As can be seen on the example of June in Figure 4-2 d, the summer months show a higher fresh water flux input across the entire Arctic. This difference can be explained by the sea ice cover in the Arctic that persists at the majority of locations throughout the majority of the year. Then, precipitation falls onto the ice instead of directly into the ocean. As a consequence, the expected positive correlation can only be observed in months without sea ice cover. This in turn means that tagging the extra

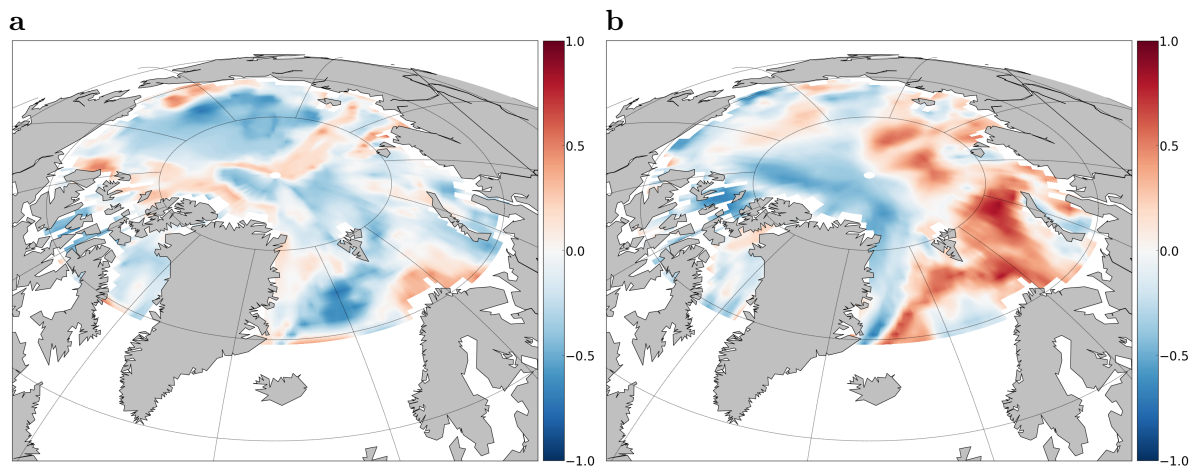


**Figure 4-1:** Pearson's correlation coefficient  $r$  between fresh water flux anomaly and salinity anomaly of scenario str relative to the control run for 20 years time series (2006-2026) of (a) Januaries and (b) Junes

fresh water volume in the Arctic, by looking at the correlation of salinity and flux anomaly, would only be achievable throughout a limited period of the year. How the sea ice model transfers ice to fresh water into the ocean cannot be deduced from the fresh water flux files. Based on these results, it became clear that it is not possible to follow the initial approach. Therefore, the approach to the question was changed, which will be outlined hereafter.

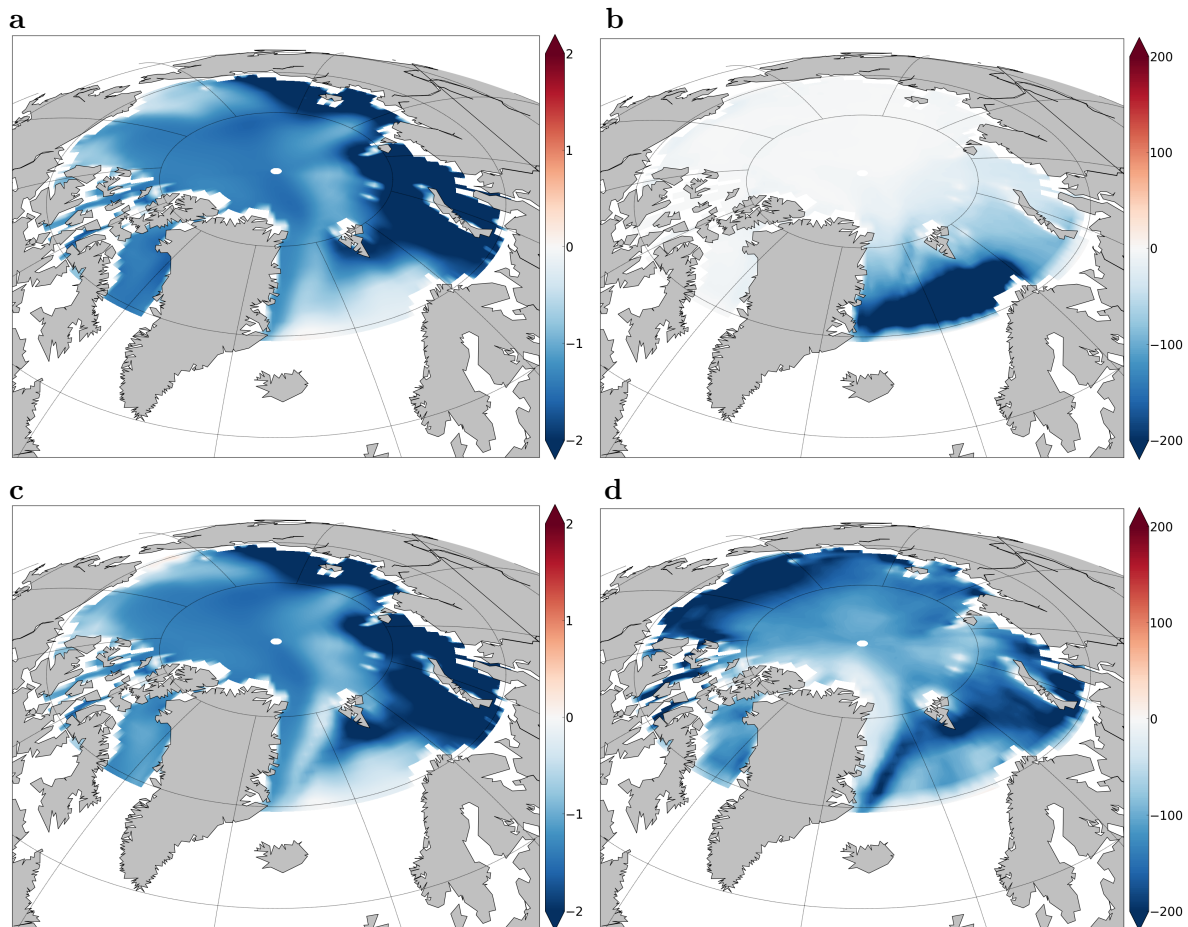


**Figure 4-2:** Average salinity [PSU] (a and c) and fresh water flux anomaly [mm/month] (b and d) for (a and b) January and (c and d) June 2006-2026 between scenario str and control run

## 4-2 Tracing Arctic Waters

The additional Arctic precipitation cannot be tagged with particles in the available model data. As outlined in Chapter 1, this research aims to explore in further detail how the extra fresh water input of the Arctic impacts ocean circulation. This means for example, shedding light on the question whether convection zones and AMOC strength are directly or indirectly affected by fresher Arctic water. Thus, as an alternative to tracing the separate fresh water volume, Arctic waters can be traced. To this end, particles were seeded in a way that all water exiting the Arctic towards the Nordic Seas could be traced. Particles were released over depth in Fram Strait (Figure 4-3). The seeding was done at  $80^{\circ}\text{N}$ , from  $-25^{\circ}\text{W}$  to  $20^{\circ}\text{E}$ , and 10 m to 4500 m depth (Figure 4-3 b). Per degree longitude 10 particles for every 20 m depth were seeded. If a particle was seeded such that it happened to be on land, CMS took the particle out of the simulation with an exit-code (this holds true for the areas coloured in red Figure 4-3 b). Particles were seeded every month for one year (in 2027). This set-up resulted into 17'980 advected particles per month, or 215'760 advected particles per year. The seeding set-up is summarized in Table 4-1. Appendix A-1-1 shows an example extract of the release file.

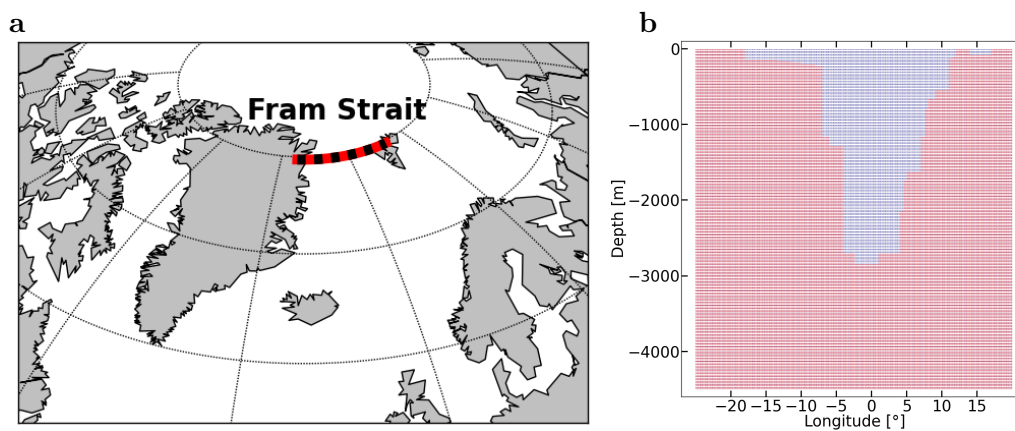


**Figure 4-3:** Seeding location at Fram Strait at 80°N - shown from (a) top view and (b) cross-sectional view. Cross-sectional view shows seeding over depth and longitude - particles coloured blue get advected.

depth [m]			longitude			latitude	particles	advected
min	max	delta	min	max	delta		[# /month]	[# /year]
10	4490	20	-25°W	20°E	0.1°	80°N	17'980	215'760

**Table 4-1:** CMS seeding input information summarized

Particles were traced for twenty years. This time span allowed to see the differences between the control run and the scenarios while not taking a very long run time in CMS. The data of 2027-2047 was used because the differences between the scenarios and the control run develop over time, and thus become more pronounced in later years (note that CMS always needs two input files in the future to finish its calculation). As already mentioned in Section 3-1-2, the oceanographic files were available in monthly intervals. The time step used for the advection in CMS was a quarter of a month. It was not chosen shorter in order to keep the run time of CMS low, and not longer for reasons of accuracy. The option of periodic boundary condition was marked as 'true' which allowed particles crossing from 179°E to -180°W. Since particles were traced forward in time, the backwards tracing module was set to 'false'. The 'avoidcoast' landmask boundary condition was set to 'true' which implies that particles cannot be wash onshore. As explained in Section 3-2-1, this is due to the fact that the particles represented water volumes as opposed to, for example, an organism. And finally, the turbulence module was set to 'false'. These run-configurations are summarized in Table 4-2. The run-configurations file can be found in Appendix A-1-2. Furthermore, Appendix A-1-3 contains the so-called nest file giving the necessary information about the data and its variable names.

#### 4-2-1 Tagging particles with transport

In order to quantify transports along different pathways, particles were tagged with their individual transport. This was done at the same time the release or seeding file was created.

start time	advection time	time step	periodic boundary condition	backward tracing	landmask boundary	turbulence module
	years	months	boolean	boolean	boolean	boolean
2027	20	1/4	true	false	true	false

**Table 4-2:** CMS Run Configurations summarized

Note that CMS does not calculate volume transports. Therefore, particles were tagged with an ID and transport before running CMS. Through the ID particles could be 'found back' in the CMS output and then they were weighted by the previously stored transport value. By adding these values up for particles that travelled the same route, the transport along that route was determined. Subsequently, the share of the transport which passed Fram Strait at the release time was calculated. Transport per particle was based on a simple linear interpolation of the horizontal velocity fields of the release time at the seeding position. Since particles were seeded at constant latitude (80°N) only meridional velocities were taken into account (v-velocities). A particle was tagged with a velocity, and subsequently transport if all grid points for interpolation were in the water (as opposed to on land). Particles outside valid grid points of the v-velocity files were not taken into account. Therefore, an error is made at the edges. However, the error is very small, and therefore negligible, since the velocity at the land boundary are close to zero. Appendix A-2 shows the transport at the cross section of Fram Strait calculated directly from the velocity fields, and as plotted from the interpolated particle values.

#### 4-2-2 Pathway categories

One of the main objectives of this study was investigate where the Arctic water passing Fram Strait travels. In order to find out which pathways exist in the model, a few sample runs were made. Based on the sample runs, four possible outcomes were identified: passing Denmark Strait, passing the Greenland-Scotland-Ridge, staying in the Nordic Seas or ending up in the Arctic. Note that there was no water passing Fram Strait that went into the Barents Sea in this model. In order to allocate particles, and therefore the respective water volume to a specific pathway, key regions were identified - see orange encircled fields in Figure 4-4. A particle was allocated to the Denmark Strait pathway if it entered box 1 during the 20 years simulation. It was allocated to the Greenland-Scotland-Ridge pathway if it passed through box 2.1 and box 2.2. If its final location was found in area 4, north of 80°N, it was assigned to the Arctic route. Particles that fulfilled neither of these criteria stayed in the Nordic Seas.

Combining the information of pathway with the volume transport of a particle, allowed the quantification of the absolute and relative share of the water passing Fram Strait per pathway. Note that to avoid double counting of volumes in these calculations, only particles were used that were travelling southwards at the initial seeding location. Particles were released 12 months in a row, meaning that e.g. a particle released in the first month which makes a loop in the Arctic and passes Fram Strait again within 12 months, would also be present in a later release month. Furthermore, the pathways were investigated with respect to their changing depth.

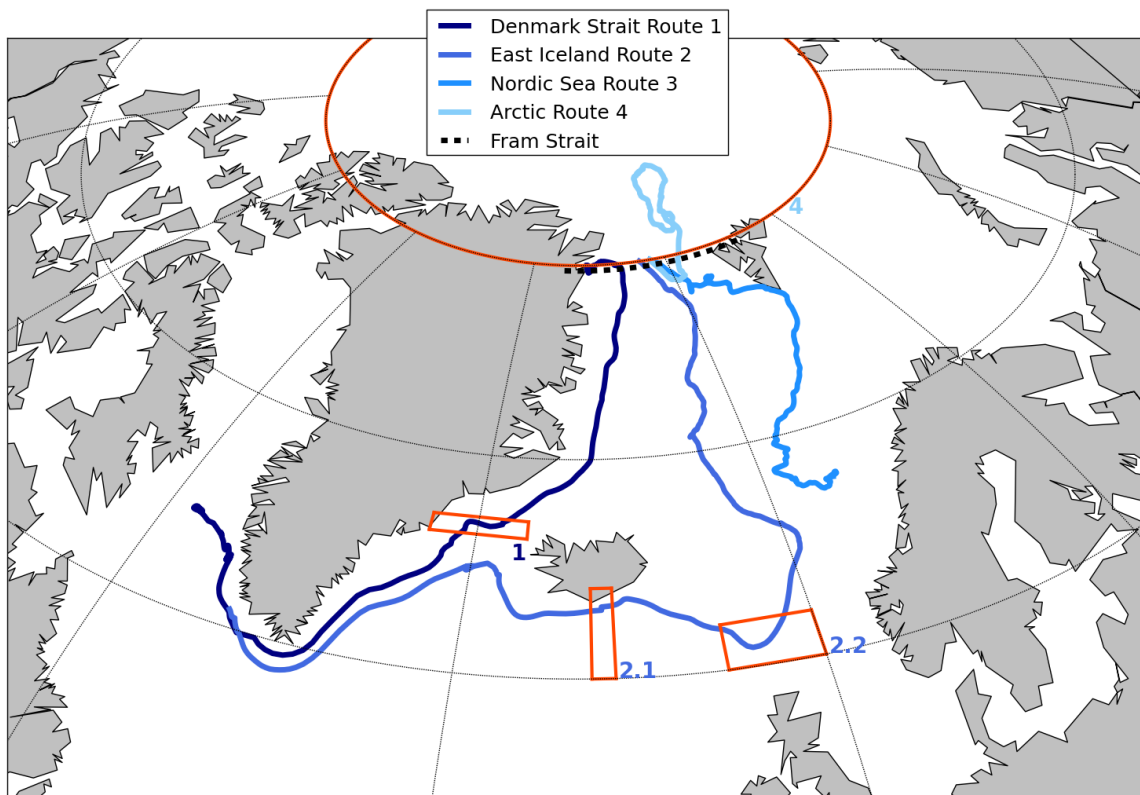


**Figure 4-4:** Pathway categories (Denmark Strait, East Iceland over the Iceland-Faroe-Ridge, Nordic Seas and the Arctic) and their allocation criteria - entering either of the respective orange area(s) as shown in figure. If a particle does not enter any of the outlined areas, it gets allocated to the pathway 'Nordic Seas'.

### 4-2-3 Analysing properties - temperature salinity

Particles of the pathways connecting the Fram Strait waters to the North Atlantic were analysed with respect to their properties, namely salinity and temperature, and the respective changes along the path. These pathways were chosen because they reach the Labrador Sea where they can influence the sinking and convection areas in place. Taking into consideration what was found in Section 5-1, three key locations were chosen for each pathway in order to compare the quantitative changes of the properties. For the Denmark Strait route, these key locations included Fram Strait, Denmark Strait and south of Greenland. For the East Iceland pathway this included Fram Strait, the Faroe Bank Channel and south of Iceland. These key locations are also marked as the selection boxes in Figure 4-4. Values for salinity and temperature within those boxes were averaged per particle. The averaged values of a particle were weighted by its transport. The weighted values of the particles of one pathway were averaged.

For the cross section at Fram Strait the density of the particles was calculated from their respective salinity and temperature values. The calculation was done for density of sea water at atmospheric pressure based on Fofonoff and Millard (1983) and Millero and Poisson (1981).



# Effects of increasing Arctic precipitation on the pathways and properties of the waters in Fram Strait

## 5-1 Pathways of the waters passing Fram Strait

As already anticipated in Section 4-2-2, the Arctic waters in EC-Earth advected 20 years from the starting position in Fram Strait could be separated into four major pathway categories - passing Denmark Strait into the North Atlantic, passing east of Iceland into the North Atlantic, ending in the Arctic or staying in the Nordic Seas. In order to add further meaning to these routes, the pathways needed to be quantified. Table 5-1 lists the absolute mean

Run	absolute transport south [Sv]	change [%]
control run	4.32	-
scenario wk	4.39	1.6
scenario str	3.48	-21.5

**Table 5-1:** Absolute transport traced southward through Fram Strait for each of the analysed runs

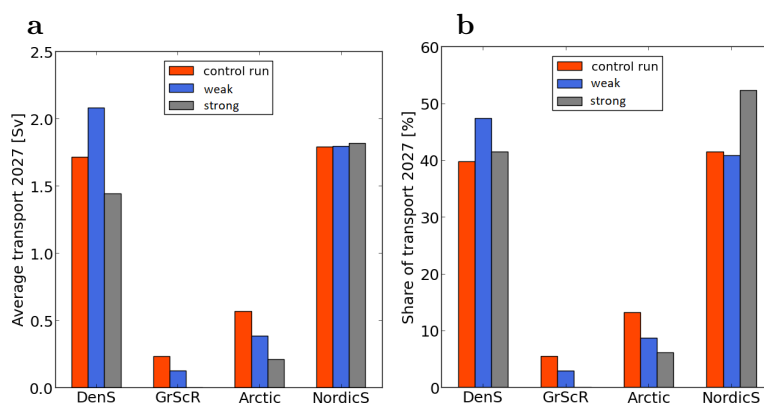


**Figure 5-1:** Mean transport in (a) absolute quantities [Sv] and (b) relative quantities [%] separated over the different pathways as defined in Figure 4-4 for each of the analysed runs (DenS = Denmark Strait, GrScR = Greenland-Scotland-Ridge, NordicS = Nordic Seas)

transport traced southward through Fram Strait found in this research. Counter-intuitively, the absolute transport southward shows a small rise for scenario wk, and a strong drop of over 20% for a scenario str. This means the quantitative response to increased Arctic precipitation at Fram Strait is not simply monotone.

Figures 5-1 a and b show how these quantities are distributed over the different pathways in absolute transport and relative shares, respectively. The quantitatively most significant pathways for the control run and the scenarios are the routes passing Denmark Strait and the pathway remaining in the Nordic Seas. Therefore, it can already be said that Arctic water passing southward through Fram Strait still passes the Denmark Strait when increasing Arctic precipitation (by 50% or 300%). Furthermore, the numbers for the absolute transports show that transports remain within the same range of magnitude as the control run. However, there was no clear monotone relation found with the amount of Arctic precipitation for the water masses staying in the Nordic Seas or passing Denmark Strait. In scenario wk the absolute amount of the water passing Fram Strait in 2027 that thereafter passes Denmark Strait is higher than in the control run, while scenario str shows lower values. This was not to be expected when looking at Figure 3-6 a, c and e. As outlined in Section 3-1-2, the water passing Denmark Strait is the modelled East Greenland current which at the uppermost surface layer gets stronger with increasing Arctic precipitation. Lower transports for scenario str suggest that this current needs to be decreasing in speed more sharply than the other two runs over depth. Therefore, the pathways were also analysed with respect to depth changes (later in this section).

The relative share of transport going through Denmark Strait shows an increase for both scenarios (Figure 5-1 b). Notably, the absolute value of water going into in the Nordic Seas, and staying for 20 years, remains almost unchanged for all three runs. Therefore, the water mass travelling from Fram Strait into the Nordic Seas might be a determining factor for the amount of water travelling from Fram Strait along the other pathways. Considering that in scenario str a lot less water travels through Fram Strait, the amount of water passing Denmark Strait needs to decrease if the amount of water staying in the Nordic Seas remains similar. This would explain why the absolute transport travelling through Denmark Strait does not simply increase with increasing Arctic precipitation. For the relative share this means however that the share of the Nordic Sea route increases notably with about 10% for scenario str. The absolute and relative numbers for the pathways towards the Arctic and over the Greenland-Scotland-Ridge decrease with increasing Arctic precipitation. The latter one even completely disappears.

To understand better why and how these quantities change, the pathways need to be scrutinized horizontally and vertically.

Figure 5-2 shows the horizontal pathways taken by the particles seeded in Fram Strait in 2027 for the control run and for the two scenarios separated by pathways. Note that these pathway-plot are not weighted with transport, but simply show the travel routes of different water masses. Figures 5-2 a-c show the particles passing Denmark Strait. It can be observed that with increasing precipitation in the Arctic the exchange between this current that passes Denmark Strait and the Nordic Seas decreases, and entirely disappears for the strong scenario. In the strong scenario the particles going through Denmark Strait take only the most direct route from strait to strait (Figure 5-2 c). While in the control run (Figure 5-2 a), particles make excursions into the Nordic Seas before crossing the strait. Figures 5-2 d-f show the pathways of the particles that enter the North Atlantic passing on the eastern side of Iceland.

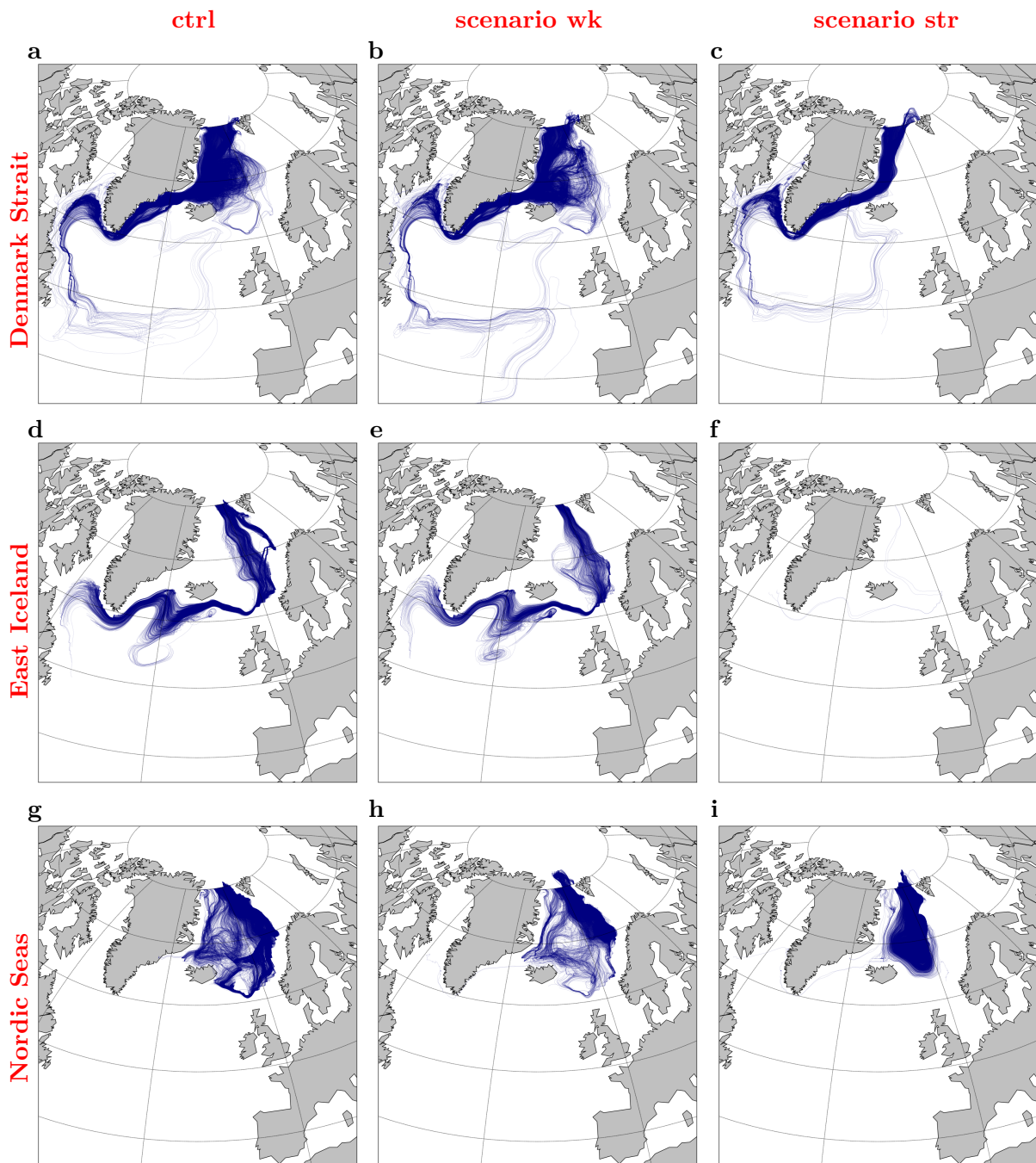


**Figure 5-2:** Horizontal pathways for 20 years advection-time of those particles seeded in Fram Strait in 2027, for (a,d and g) the control run, (b,e and h) scenario wk and (c,f and i) scenario str, which fall into one of the three categories: (a-c) passing Denmark Strait, (d-f) passing east of Iceland over Iceland-Faroe-Ridge or (g-i) staying in the Nordic Seas (note that those particles ending up in the Arctic are not shown since their pathways are less relevant to this study)

As already visible in Figure 5-1, this pathway completely disappears in the strongest scenario (Figure 5-2 f). Figures 5-2 g-i show the pathways of those particles staying in the Nordic Seas after 20 years of advection. Also here it can be observed that the pathways are a lot more compact in the strongest scenario (Figure 5-2 i) than in the control run and in scenario wk (Figures 5-2 g and h respectively). In the control run and scenario wk there are several particles which are about to cross Denmark Strait after having stayed 20 years in the Nordic Seas. This shows that particles having spent some time in the Nordic Seas are still able to cross Denmark Strait. In scenario str there are hardly any particles crossing the strait after the same amount of time. The fact that the particles get more confined to their specific pathway with increased Arctic precipitation does suggest that the different pathways start being confined to different depth ranges. Note that this could also be a cause of the disappearance of the route around East Iceland - if this route depends on depth changes. The latter is likely since this pathway should be representing overflow. Therefore, the following is dedicated to an analysis of the particles' depth for the three different runs.

Figure 5-3 shows the starting position at the first time step (= the seeding location at Fram Strait at  $80^{\circ}\text{N}$ ), color-coded according to the separation by pathway shown in Figure 5-2 for all three runs. The pathway 'Arctic' was assigned to particles ending in the Arctic (north of  $80^{\circ}\text{N}$ ) after 20 years of advection (this includes particles going initially south and those going directly north). Particles of this pathway are coloured turquoise. For the control run (Figure 5-3 a), particles starting below 1300 m depth will end up in the Nordic Seas after 20 years of advection (dark blue). A few exceptions are coloured dark red and will pass the Greenland-Scotland-Ridge. Particles seeded between about 800-1300 m depth take different routes depending on their longitudinal position. The majority of these particles is coloured dark blue and ends in the Nordic Seas. However, the ones seeded on the more western half of the strait pass the Greenland-Scotland-Ridge (dark red) and the Denmark Strait (orange, this route is travelled by the ones seeded at the most western edge of the strait). From about 250-800 m particles will end up in the Arctic (turquoise) or, if seeded on the western edge go through Denmark Strait (orange). The bulk of particles seeded at the surface end up going through Denmark Strait (orange). The orange particles going through Denmark Strait travel as part of the East Greenland Current (see Section 2-1). A few particles seeded at the

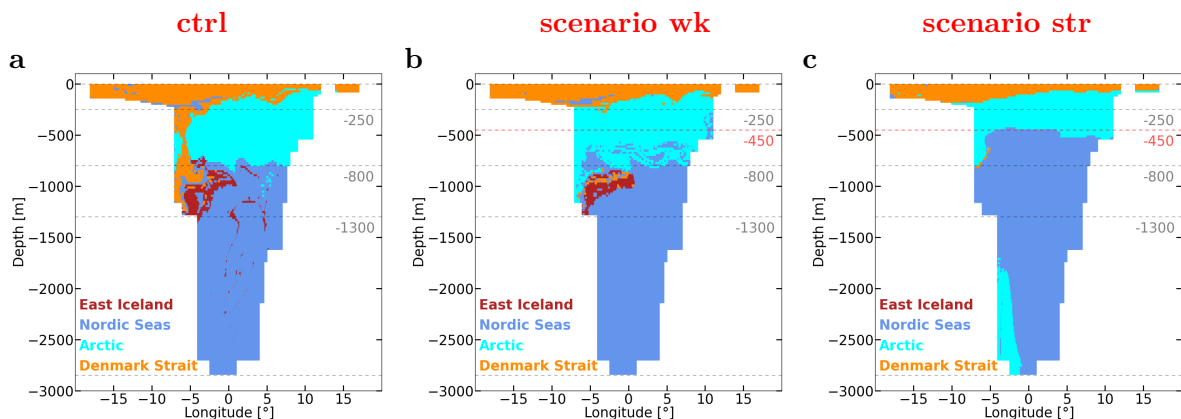


**Figure 5-3:** Particle positions at first time step in the cross section of Fram Strait at  $80^{\circ}\text{N}$  (= seeding location plotted over depth and longitude) color-coded by the pathway they take during 20 years of advection for (a) the control run, (b) scenario wk and (c) scenario str

western side of this surface layer end up in the Nordic Seas (dark blue) and a few seeded at the eastern side of this surface layer end up in the Arctic (turquoise).

Increasing the Arctic precipitation by half (scenario wk, Figure 5-3 b) causes some changes. Notably, those particles seeded between 200-1300 m depth at the western edge of the strait change destination from Denmark Strait to the Arctic. Furthermore, more pathways above 800 m depth lead to the Nordic Seas instead of travelling to the Arctic. Between 800-1300 m there is still a larger patch of dark red particles taking the route over the Greenland-Scotland-Ridge, but below 1300 m depth no particles take this route anymore. In line with what was shown in Figure 5-2, there seems to be less interaction between the different routes when considering increased Arctic precipitation. For the strong scenario, edges between the different groups of particles taking specific routes are sharper (Figure 5-3 c). The patches of the start position of particles going the same direction are more defined and confined to one area instead of being scattered about. The surface layer of orange particles taking the Denmark Strait route becomes shallower. This suggests that especially the extra fresh water of the Arctic will enter the North Atlantic, since the extra precipitation can be expected in the surface layer. However, this needs to be scrutinized further, which will be done in Section 5-2. The entire layer of turquoise particles below this surface layer end up in the Arctic. The upper edge of the patch of dark blue particles going to the Nordic Seas is raised from about 800 m depth in the control run to about 450 m depth. Furthermore, there is a new group of turquoise particles at the western side of the strait, from about 1800 m depth to the bottom going to towards the Arctic instead of the Nordic Seas.

In this series of plots scenario wk seems to show a sort of transition phase between the control run and scenario str. The patches formed by particles of the same pathway get increasingly ordered into horizontal layers. This seems to indicate an intensifying stratification of the strait and the Nordic Seas. The latter can be assumed due to the fact that there are hardly any particles left in the strong scenario which were seeded below 210 m depth that cross into the North Atlantic. The path east of Greenland even completely disappears. That implies further that particles cannot change depth sufficiently in the Nordic Seas any longer in order to cross Denmark Strait or the Greenland-Scotland-Ridge. Water masses change depth with changing density (relative to the surrounding water column), and density of a water mass alters with changing temperature and salinity. These properties can change either due to interaction with the atmosphere or within the mixed layer depth. As could be seen in Figure 3-4, the mixed layer depth decreases drastically in the Nordic Seas with increased Arctic precipitation. Therefore, it seems logical to assume that for scenario str (and partly scenario wk) particles are not changing properties (and therefore density) to an extent that they can change depth range sufficiently in order to maintain the route over the Greenland-Scotland-Ridge and parts of the route through Denmark Strait. In order to check this explanation further, the temperature, salinity and depth change along the particle trajectories need to be scrutinized. The analysis of the properties can be found in Section 5-2 and the depth analysis follows here.

Figure 5-4 again shows particle trajectories of each model run, but with an additional colour coding indicating the depth of the respective particle and its location. Figures 5-4 a-c show the pathway of the particles passing Denmark Strait for each run respectively. Most strikingly, for all three runs the particles sink by several hundreds of metres after passing the southern tip of Greenland. Yet, when looking at the Labrador Sea, more pathways take shallower routes on the edges of the main pathway with increasing Arctic precipitation. This is most visible in Figure 5-4 c on the northern side of the current in the Labrador Sea. When

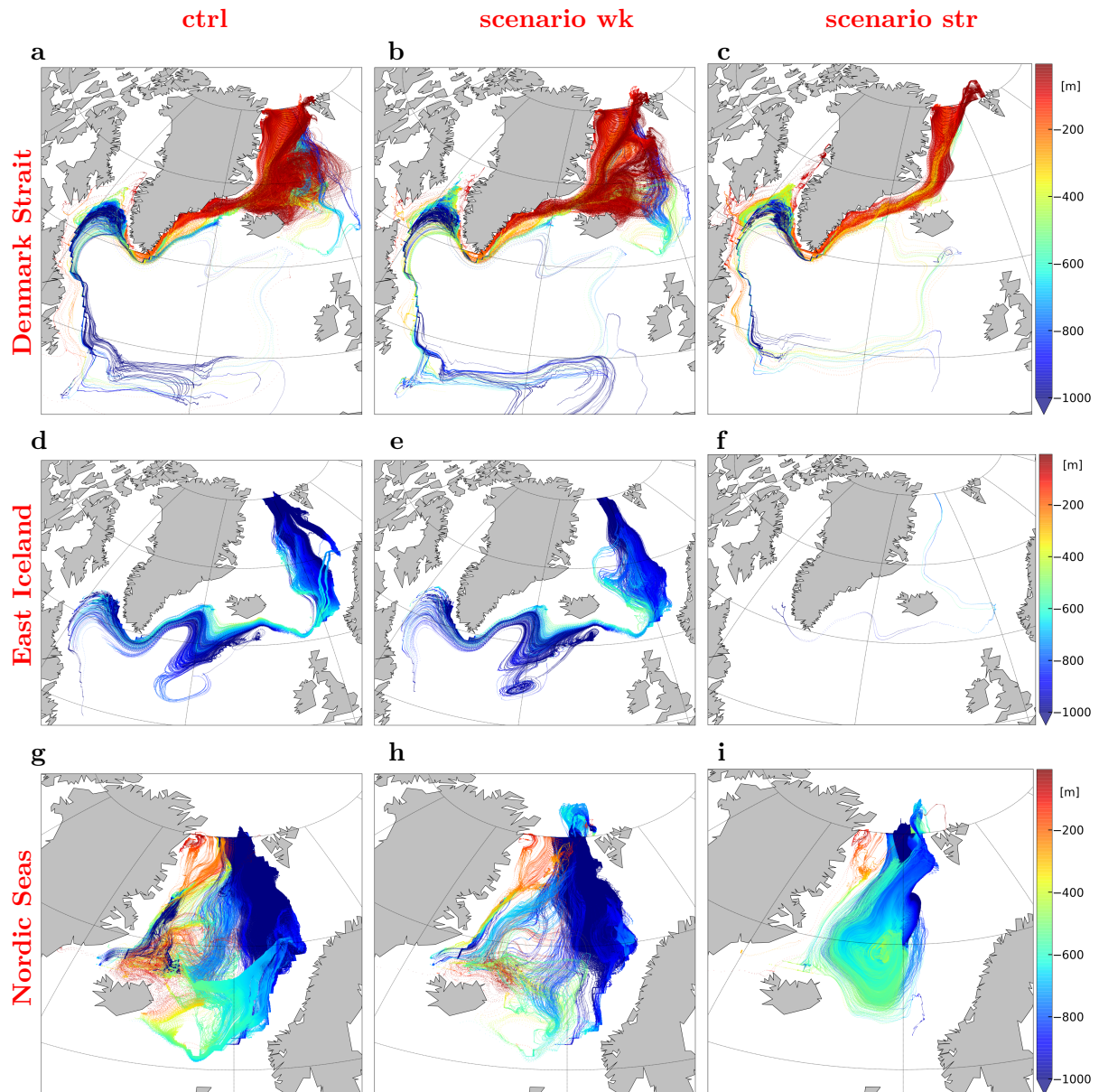


**Figure 5-4:** Pathways for 20 years advection-time of those particles seeded in Fram Strait at  $80^{\circ}\text{N}$  in 2027, for (a,d and g) the control run, (b,e and h) scenario wk and (c,f and i) scenario str, which fall into one of the three categories: (a-c) passing Denmark Strait, (d-f) passing over Iceland-Faroe-Ridge or (g-i) staying in the Nordic Seas. Color-coding illustrates the depth [m] along the respective pathway. (Note that this figure is the same as Figure 5-2 with an added colour-coding for depth)

looking closely at the stretch between Denmark Strait and the southern tip of Greenland for the control run (Figure 5-4 a), the dark blue coloured pathways let assume that there is an overflow at depth of the strait below the main pathway at the surface. For scenario wk (Figure 5-4 b), this deep part of the pathway becomes shallower and less travelled, and for scenario str (Figure 5-4 c), it almost disappears. Furthermore, it can be seen clearly that in the control run and scenario wk (Figures 5-4 a and b), some of the particles enter the Nordic Seas at depth and then rise again and pass Denmark Strait. These excursions into the Nordic Seas completely disappear for the strong scenario (Figure 5-4 c). Since the water masses passing Denmark Strait play a key role for the sinking and convection zones in the Labrador Sea, this will be looked at more closely in Subsection 5-1-1. This disappearance of vertical interaction supports the argument from above.

Figures 5-4 d-f show the depth-colour-coded route passing the Greenland-Scotland-Ridge. For the control run and scenario wk, the behaviour of the particles look quite similar from this perspective (Figure 5-4 d and e respectively): from around thousand metres depth, they enter the Nordic Seas where they rise slightly in the water column and subsequently pass Greenland-Scotland-Ridge as overflow. As could be seen in Figure 5-3, these water parcels started for both runs at around 800-1300 m depth in Fram Strait. As Figure 5-2 f already showed, for the strong scenario this route ceases to exist (Figure 5-4 f). This result also reinforces the explanation outlined above. The particles passing into the North Atlantic via the east of Iceland represent overflow over the Greenland-Scotland-Ridge. That overflow depends on particles being able to relatively change their density such that they raise in the water column sufficiently in order to pass the ridge. This is not possible in scenario str.

Figures 5-4 g-i show the depth-colour-coded pathways for the particles staying in the Nordic Seas. It can be observed that depth range of particles becomes more homogeneous with increasing Arctic precipitation. The control run (Figure 5-4 g) shows the least homogeneous situation, with particles changing their depth significantly and travelling many different routes. Particles change their depth less in scenario wk (Figure 5-4 h). And when looking at scenario str (Figure 5-4 i) particles change depth significantly less - they all stay on similar routes. The bulk of pathways is more compact, not just in the horizontal but also in the vertical. Yet, as already seen in Figure 5-3 there are particles at decreased depth staying in the Nordic Seas. Again, this shows the increased stratification, causing less deep interaction between layers and therefore trajectories.

### 5-1-1 Denmark Strait - a closer look

Since the overflow of Arctic water at Denmark Strait seems to disappear (Figure 5-4 a-c, Section 5-1), this subsection will show some more insight of the situation at Denmark Strait. This can be seen more clearly in Figure 5-5, which shows a zoom in on Denmark Strait's depth-colour-coded pathways. In Figure 5-6 a-c the distribution of the particles over depth and longitude is shown for each run respectively. When comparing the control run and scenario wk, several changes can be observed. In the control run many particles pass the strait at the surface at its most western side. In scenario wk this changes to a bias toward the surface stretch in the middle of the Strait. On the eastern edge towards the bottom (below 400 m depth and between  $-27^{\circ}\text{W}$  and  $-26^{\circ}\text{W}$ ) the density of pathways decreases notably from the control run to scenario wk. At mid-depth, around 300-350 m at about  $-32^{\circ}\text{W}$  and  $-31^{\circ}\text{W}$ , scenario wk shows an increased density of particles compared to the control run. In

scenario str the route at the most western surface (upper 80 m) almost entirely disappears. But in contrast to scenario wk they do not redistribute towards the surface in the middle of the strait, but spread out a bit further east at about 50-200 m depth. At the eastern bottom, particle density decreases even more and at the western edge at around 300-350 m depth the density increases even more than in scenario wk compared to the control run.

When looking at the absolute transports these particles represent, strong western surface currents can be seen for the control run and scenario wk. As the particle density of scenario str already indicated, this surface current redistributes further east and sinks to about 50-200 m depth. Furthermore, transports below 400 m depth, still visible for the control run and scenario wk, disappear in the strong scenario. In the latter one in contrast, the western current at mid-depth intensifies (at 300-350 m depth).

Arctic water overflowing the Denmark Strait decrease with increasing Arctic precipitation. This result gives another reason to look into the properties along the pathway of the modelled East Iceland current.

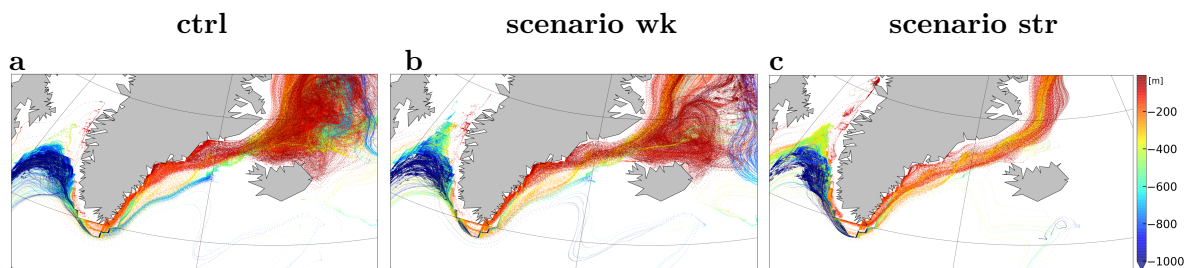


**Figure 5-5:** Zoom in on pathways crossing Denmark Strait color-coded according to depth for (a) the control run, (b) scenario wk and (c) scenario str respectively (= zoom in on Figure 5-4 a-c)

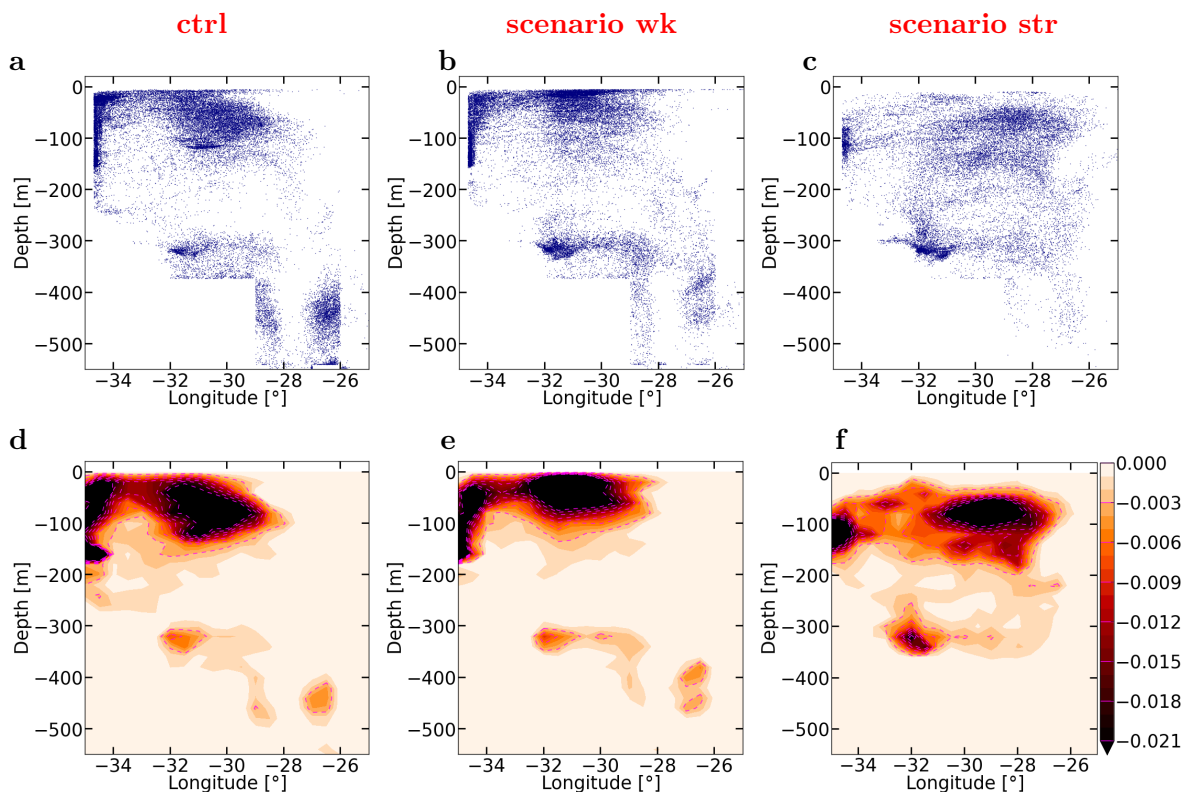


**Figure 5-6:** Particle distribution (a-c) and respective transport distribution [Sv] (d-f) in the cross section of Denmark Strait. Transport is allocated and plotted over depth and longitude based on a grid of 20 m depth by  $0.1^\circ$  longitude.

## 5-2 Properties of the traced water masses

### 5-2-1 Properties of the Arctic waters passing Fram Strait

The results of the quantitative 3D-pathway analysis performed in Section 5-1, show that the extra Arctic precipitation changes alter the water properties such that the pathways of the Arctic water passing Fram Strait change strength, depth or even entirely disappear. Therefore, several aspects concerning temperature and salinity of the traced water particles and their respective changes were analysed. First of all, Figure 5-7 shows the initial seeding properties. It becomes clear that the properties of the water passing Fram Strait changes. Figures 5-7 a-c show the salinity for (a) the control run, (b) scenario wk and (c) scenario str. The extra fresh water at the surface is clearly visible in the scenarios (b and c) compared to the control run (a). This was to be expected because of the extra fresh water input at the surface in form of precipitation for the scenario runs. However, the freshening can also be observed at depth. In the control run, an area at 1000-2000 m depth exists which is fresher than the layer above (Figure 5-7 a). It is thicker on the western boundary of the strait. The layer above shows saltier values and is thicker at the eastern boundary of the strait. This saltier layer gets thinner for scenario wk and completely disappears in scenario str. Scenario str shows a gradual layering from salty at the bottom to fresh at the surface. This indicates again the increasing stratification for the scenario runs.

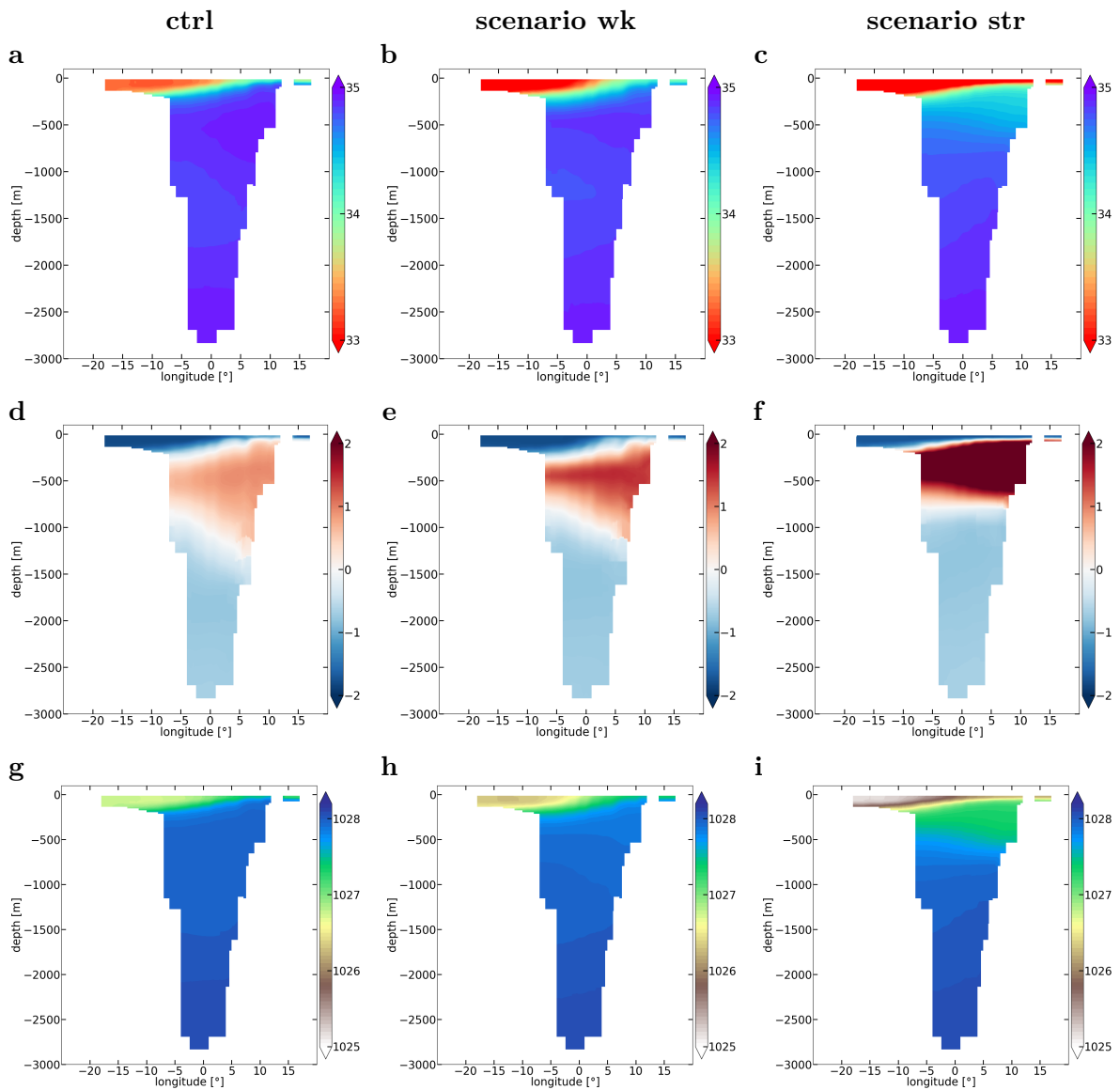


**Figure 5-7:** Salinity [PSU] (a-c), Temperature [°C] (d-f) and Density [ $kg/m^3$ ] (g-i) of particles seeded in Fram Strait at  $80^\circ N$  over depth and longitude for (a,d and g) the control run, (d,e and f) scenarios 5 and (c,f and i) scenario str. Temperature and Salinity values are taken at first time step of the CMS calculations and the respective density values are calculated.

Figures 5-7 d-f show the temperature values of the particles seeded in Fram strait for (d) the control run, (e) scenario wk and (f) scenario str. Interestingly, also the temperature values change for the scenario runs - noting once more that the only thing changed for the scenario runs was the extra precipitation over the Arctic. In the control run a triangle shaped area can be observed reaching up to around 1400 m depth. For scenario wk, the shape of the triangle stays roughly the same, but the area gets warmer. Scenario str, shows a more extreme change, which the triangle flattened out to a more rectangular shaped layer and increasing its temperature even more. The surface layer is coldest for all three runs. The cold layer decreases in thickness with increasing precipitation.

Figures 5-7 g-i show the calculated densities from the salinity and temperature values for (g) the control run, (h) scenario wk and (i) scenario str. While in the control run a very similar density between 400 m and 1500 m depth can be seen, the vertical density gradient increases with increasing Arctic precipitation for the scenario runs. The area between around 200 m to 1000 m depth is changing most notably. As described it becomes less salty and warmer which means the density decreases strongly. Again this leads to a stabilisation of the water column. The increasing stratification prevents particles from moving up and down in the water column. This in turn allows explaining why particles released deeper than the deepest point of Denmark Strait stop crossing the ridge, as was shown in Figure 5-3. Though looking at the properties of particles, it is needless to say that this is an Eulerian view of the starting position. It shows the stratification at a certain place, Fram Strait cross section, at a certain moment in time, the release time. This is of course valuable knowledge which allows making assumptions as to why particles travel the way they do. Yet, as explained in Section 3-2-1, the Lagrangian view allows observing the change of these particular water volumes of interest for the entire 20 years advection time.

## 5-2-2 Changing properties along pathways

So far only the particle-properties of the starting location have been shown. The Lagrangian view allows following the evolution of these properties. It should be emphasised once more that this means looking at the same water volume over time. Depending on where it is located, its properties can change. An analysis of these changes along path has been done for the pathway passing Denmark Strait and the pathway passing East Iceland. The focus has been laid on these two pathways, because along these routes Arctic water ultimately reaches the North Atlantic and the Labrador Sea. As explained in Section 2-1, the Labrador Sea is of major importance to the AMOC since there are important sinking locations and convection zones.

### Denmark Strait route

Figure 5-8 shows the Denmark Strait pathway color-coded for salinity (Figures 5-8 a-c) and temperature (Figures 5-8 d-f) for (a and d) the control run, (b and e) scenario wk and (c and f) scenario 4. In general it can be said that the pathways become fresher with increasing Arctic precipitation. The temperature shows only minor changes between the different runs, though scenario str gets a little warmer. When looking at the overflow at Denmark Strait identified in Section 5-1-1 (dark blue stretch right after Denmark Strait in Figure 5-5 a, getting less

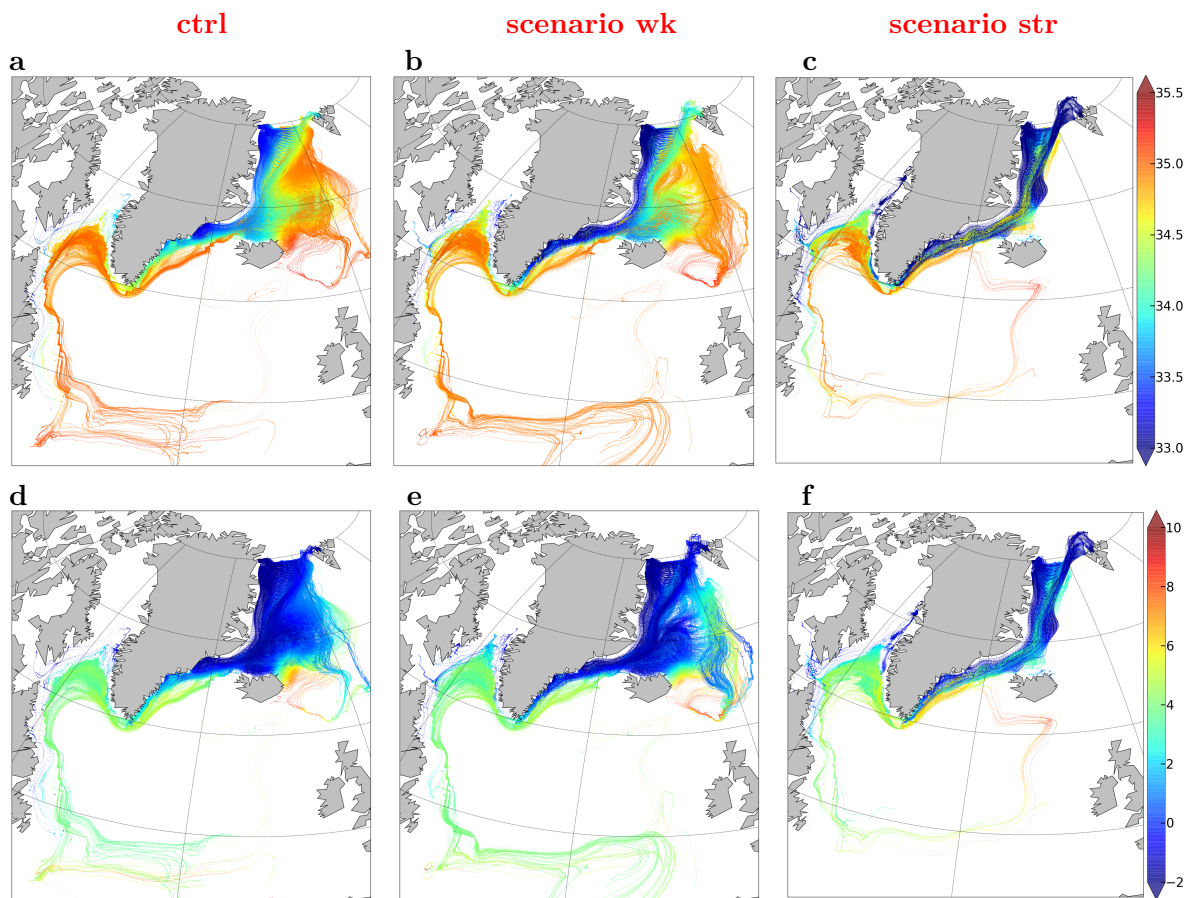


**Figure 5-8:** Salinity [PSU] (a-c) and Temperature [°C] (d-f) along the horizontal pathways of particles seeded in Fram Strait that pass Denmark Strait for (a and d) the control run, (d and e) scenario wk and (c and f) scenario str

pronounced in Figure 5-5 b and c), it can be seen that the deep current is saltier and a little warmer than the surface current. Thus, the higher salinity seems to be the reason for these particles travelling at depth. As becomes obvious, Figure 5-8 shows the general trend of the property development of the pathways, but in order to state things with certainty the changes need to be quantified and weighted with transport.

To this purpose three locations were chosen in order to be compared: Fram Strait, Denmark Strait and the southern tip of Greenland. Fram Strait and Denmark Strait are obvious choices, since they represent the connection between the Arctic and the Nordic Seas and between the Nordic Seas and the North Atlantic respectively. The southern tip of Greenland was chosen because Figures 5-5 a-c show that many particles sink drastically after having passed here. It is also the entry location into the Labrador Sea. Figure 5-9 illustrates the location choices and the values which were compared for an example particle. Figure 5-9 a shows the three locations on the map. For the tip of Greenland and Denmark Strait orange boxes show the areas which are used to allocated values to the respective location. For the example-particle these values are coloured in pink. For the Fram Strait the first five time steps were used (also highlighted in pink). Figure 5-9 b shows the properties salinity, temperature and depth of the same example particle over time. The time periods when the particle is located at one of

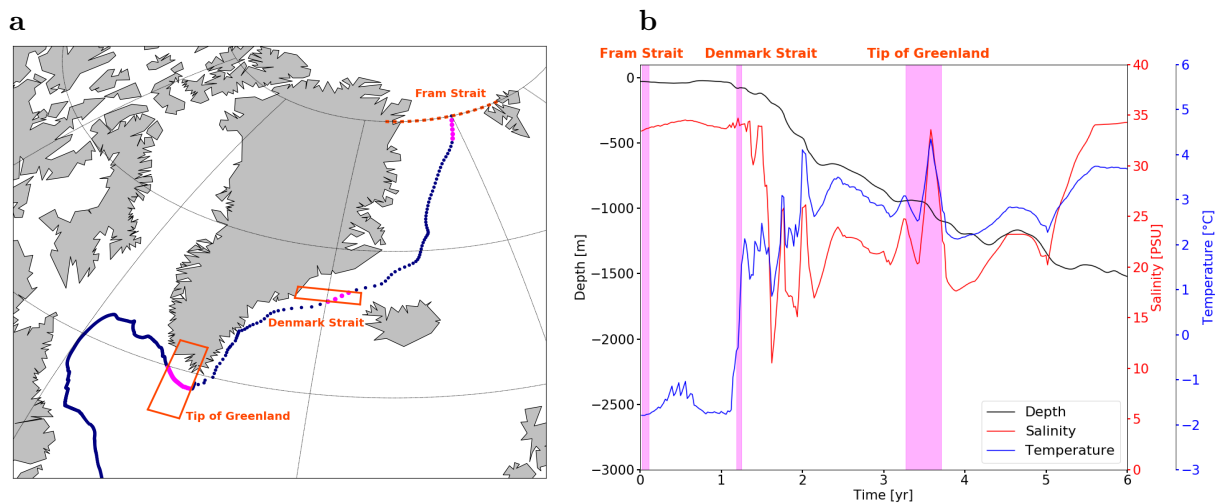


**Figure 5-9:** Explanatory figure that shows the pathway of one example-particle from Fram Strait to the Labrador Sea passing Denmark Strait (a). The values of three key locations (Fram Strait, Denmark Strait and the most southern tip of Greenland) are highlighted in pink. Plot b shows the properties salinity [PSU], temperature [°C] and depth [m] of the same particle over time. The values at the time when the particle is at the key locations, as shown in plot a, are again highlighted in pink.

the key locations are highlighted in pink. The values for temperature and salinity which were found in the highlighted areas were averaged for each of the three locations, resulting in one temperature and one salinity values per location. This was done for all the particles crossing Denmark Strait. Subsequently, these values were weighted with the transport of the particle and summed up. In a second step the changes between the key locations were calculated. This was done for all three runs. The results can be seen in Figure 5-10 for temperature and in Figure 5-10 for salinity.

Figure 5-10 a shows the mean temperature at the three key locations Fram Strait, Denmark Strait and the southern tip of Greenland for all three runs. The Arctic water passing Denmark Strait of scenario wk shows for all three locations the coldest values. In Denmark Strait the Arctic water is still below zero. Interestingly, in scenario wk, as can be seen in Figure 5-10 b, the Arctic water traced warms the least of the three runs between Fram Strait and Denmark Strait, but it warms the most in the stretch between Denmark Strait and the tip of Greenland. This makes sense because the water mixes after Denmark Strait with the warm and salty currents in the North Atlantic. The temperature difference between the Arctic water passing Denmark Strait and the warm currents of the North Atlantic must therefore be the highest in scenario wk of the three runs. When looking only at those particles reaching the tip of Greenland, they warm up the least over the entire journey in scenario wk. Scenario str shows colder temperatures than the control run at Fram Strait (Figure 5-10 a). At Denmark Strait and the tip of Greenland, temperatures are warmer than in the control run. Notably, for these location at Denmark Strait and the southern tip of Greenland scenario wk showed lower temperatures than the control run. Thus, for the temperature of the Arctic waters passing Denmark Strait, the increasing Arctic precipitation does not trigger a general trend of decreasing or increasing values. In Figure 5-10 b it can be seen that scenario str warms the most between Fram Strait and Denmark Strait, but the least between Denmark Strait and

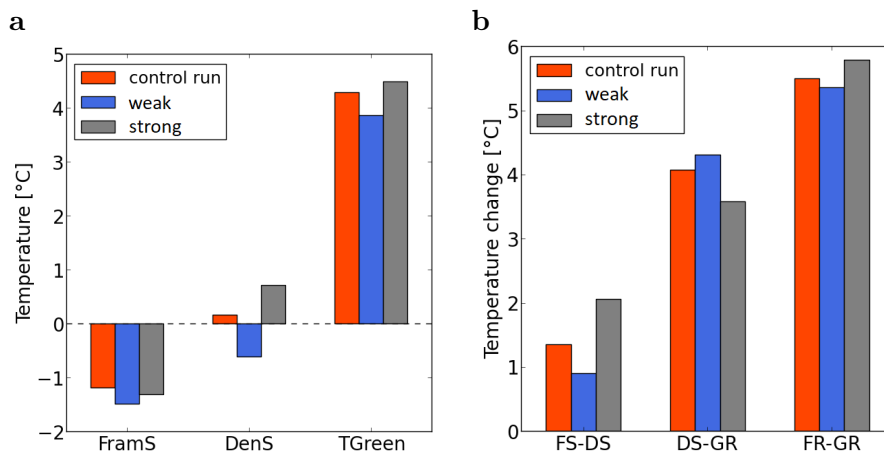


**Figure 5-10:** Mean temperature [°C] of the Arctic waters passing Denmark Strait at three key locations (FramS = Fram Strait, DenS = Denmark Strait, TGreen = southern tip of Greenland) for the control run, scenario wk and scenario str (a). And temperature changes [°C] between the respective key locations for all three runs (b)

the southern tip of Greenland. This makes sense for the same reason as for scenario wk. The waters will mixed with the warmer North Atlantic currents, but the discrepancy between the temperatures of the two currents mixing are in this case smaller than for the other two runs. When looking only at those particles reaching the tip of Greenland, they warm up the most over the entire journey in scenario str. Some of these things can be explained with the fact that water masses only change their properties in the mixed layer depth or at exposure to the atmosphere. As could be seen in Figure 3-4, the mixed layer depth decreases in the Nordic Seas with increasing Arctic precipitation. This could be the reason the Arctic waters crossing Denmark Strait warm up less in the Nordic Seas for scenario wk compared to the control run. That the opposite is the case for scenario str can be explained with Figure 5-3, which shows that for scenario str the particles crossing Denmark Strait are the most confined to the surface of all three runs. Thus, for this scenario, the heat exchange with the atmosphere could play the most important role for the temperature change of the particles crossing Denmark Strait.

Figure 5-11 a shows the salinity values of the three key locations for all three runs. In contrary to what was seen for the temperature values, salinity does respond for both scenario runs with the same trend for increasing Arctic precipitation. For both scenarios salinity decreases at all locations compared to the control run. As expected due to mixing with the more saline North Atlantic currents, the southern tip of Greenland shows for all three runs the highest salinities. Notable is the relatively high difference of scenario str at Fram Strait compared to the two other runs. This is a direct response to quadrupling Arctic precipitation in this run, since the particles crossing Denmark Strait in scenario str are found at the surface (Figure 5-3 c). However, at Denmark Strait, though still fresher, this high discrepancy has disappeared. This can also be found back in Figure 5-11 b. The Arctic water crossing Denmark Strait in scenario str increases its salinity by almost 1 PSU between the Denmark Strait and Fram Strait. In contrary, the control run and scenario wk freshen slightly over the same stretch. For all stretches shown in Figure 5-11 b scenario str freshens the most.

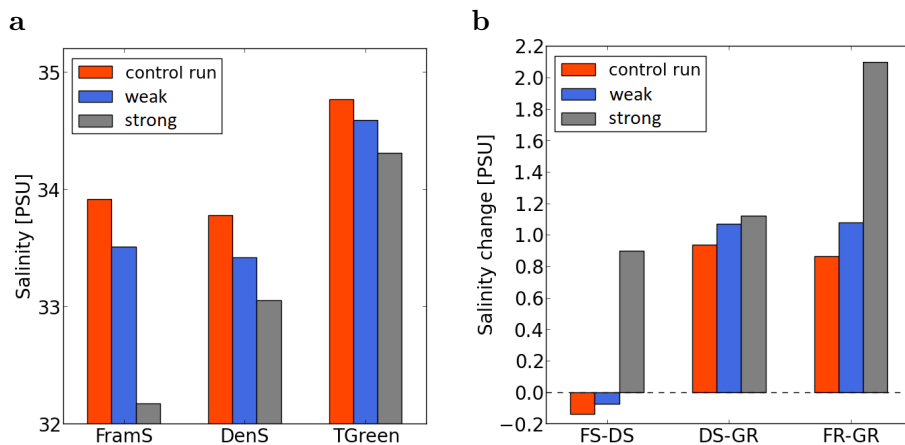


**Figure 5-11:** Mean salinity [PSU] of the Arctic waters passing Denmark Strait at three key locations (FramS = Fram Strait, DenS = Denmark Strait, TGreen = southern tip of Greenland) for the control run, scenario wk and scenario str (a). And salinity changes [PSU] between the respective key locations for all three runs (b)

### East Iceland route

Figure 5-12 shows the East Iceland pathway color-coded for salinity (Figures 5-12 a and b) and temperature (Figures 5-8 c and d) for (a and c) the control run and (b and d) scenario wk.

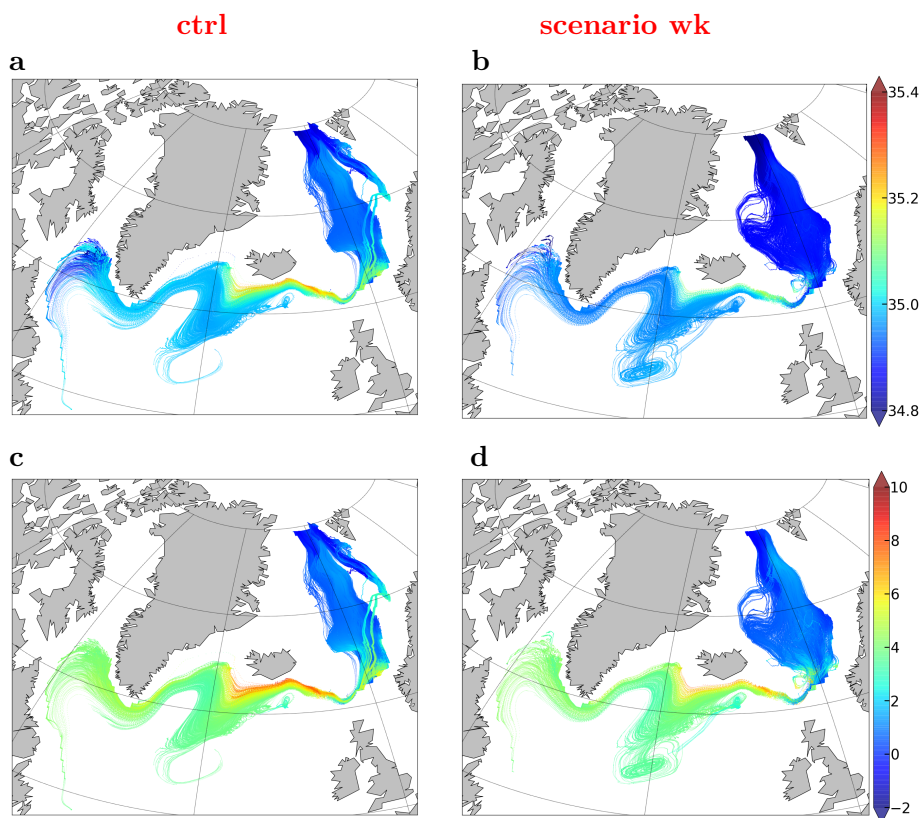


**Figure 5-12:** Salinity [PSU] (a and b) and Temperature [°C] (c and d) along the horizontal pathways of particles seeded in Fram Strait that pass Iceland Faroe Ridge for (a and d) the control run and (d and e) scenario wk.

As was seen in Figure 5-2 f, for scenario str this route does not exist. Figures 5-12 a-d show the general trend of how the salinity and temperature develop along the pathway. For both, control run and scenario wk, particles get saltier (Figure 5-12 a and b respectively) and warmer (Figure 5-12 c and d respectively) in the Nordic Seas. As is known of Figure 5-4 d and e, particles taking this route rise in the water column within the Nordic Seas to then subsequently cross through the Faroe Bank Channel. Considering this information combined with the changes in properties, the warming of the Arctic water must play the crucial role for the decrease in density allowing the crossing of the Faroe Bank Channel. After the channel, as is also known from Figure 5-4 d and e, the more northern particles stay at about the same depth of around 600 m until reaching the southern tip of Greenland. Though, the majority of pathways start sinking to greater depths after the Channel. As can be seen in Figure 5-12 a and b show that the salinity of particles increases after the channel for both, the control run and scenario wk. The more northern particles remaining at the same depth increase more notably which is counter intuitive considering what we know about sinking. Figure 5-12 c and d show that the all particles get warmer. Also here, the once the more northern once remaining at the same depth increase their temperature more notably than the rest. Thus, again temperature must play the crucial role for particles to sink or not after the channel. The more visible changes after the channel is due to the mixing with the North Atlantic currents that are warmer and more saline. All these changes are slightly less pronounced in scenario wk compared to the control run. As already done for the Denmark Strait pathway, the changes need to be quantified and weighted by transport. This allows for more accurate knowledge about what happens to the Arctic waters taking the East Iceland route into the North Atlantic.

Figure 5-13 shows the same explanatory illustration of the quantitative property analysis for the East Iceland route as Figure 5-9 does for the Denmark Strait route. Figure 5-13 a visualises the three key locations chosen for this route: Fram Strait, the Faroe Bank Channel and the South of Iceland. Again Fram Strait and the Faroe Bank channel connect different ocean basins: the Arctic to the Nordic Seas and the Nordic Seas to the North Atlantic Ocean

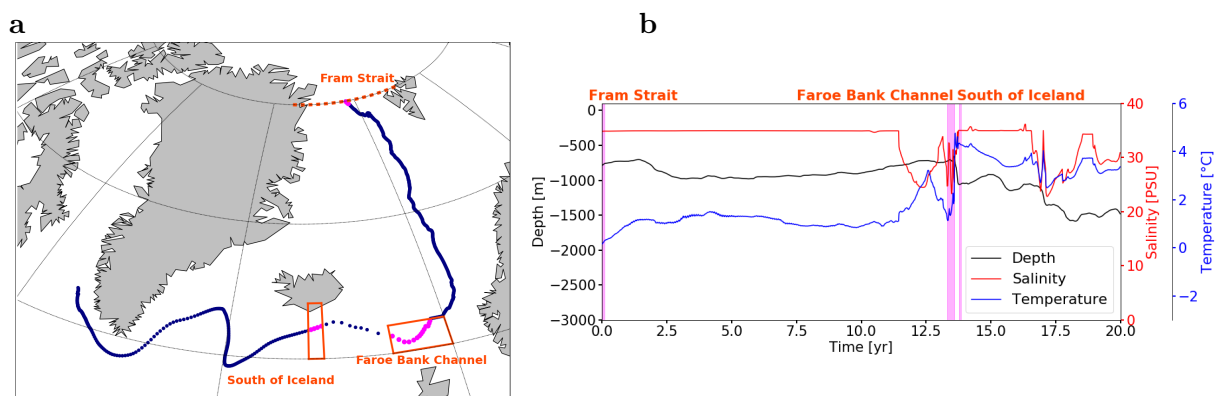


**Figure 5-13:** Explanatory figure that shows the pathway of one example-particle from Fram Strait to the Labrador Sea passing the Faroe Bank Channel (a). The values of three key locations (Fram Strait, Faroe Bank Channel and south of Iceland) are highlighted in pink. Plot b shows the properties salinity [PSU], temperature [°C] and depth [m] of the same particle over time. The values at the time when the particle is at the key locations, as shown in plot a, are again highlighted in pink.

respectively. The southern part of Iceland was chosen because Figure 5-4 d and e show that by the time particles pass here, a big share of them already sunk again. This can be due to the relative change of density to the surrounding water masses (Nordic Seas vs North Atlantic), or a direct change of properties of the volume of water the particle represents. Figure 5-13 b shows the change of the properties temperature, salinity and depth over time for the example-particle. The values for the time periods the particle spend at the key locations are highlighted in pink. Again, the values for temperature and salinity were averaged for each particle at the three locations, resulting in one temperature and one salinity value per particle and location. This was done for all the particles taking the East Iceland route. The transport-weighted sum of these properties for each location and run are found in Figure 5-14 a for temperature and Figure 5-15 a for salinity. The changes between the key locations for each run are found in Figure 5-14 b for temperature and Figure 5-15 b for salinity. Figure 5-14 a shows that the temperature of the particles travelling the East Iceland route is almost identical for the control run and scenario wk. However, at Faroe Bank Channel and the south of Iceland the temperature of the same particles in scenario wk is on average lower than in the control run. In both runs, the particles first get warmer between Fram Strait and the Faroe Bank Channel and then cool down on the stretch between the Faroe Bank Channel and the south of Iceland. The absolute changes are shown in Figure 5-14 b. More detailed, it shows that for scenario wk particles first warm up less between Fram Strait and the Faroe Bank Channel compared to the control run, and subsequently cool down more between the Channel and the south of Iceland compared to the control run. These changes allow explaining what was shown in Figure 5-4 d and e. Particles rise in the water column within in Nordic Seas, cross the Faroe Bank Channel and sink again. The warming of the particles in the Nordic Seas, lowers the density and therefore can be an explanation for particles being able to change depth to cross into the North Atlantic. Then particles get generally colder again which increases the density and allows them to sink.

Figure 5-15 a shows that the difference in salinity between scenario wk and the control run is quite small. At Fram Strait the control run is less than 0.1 PSU more saline. The difference

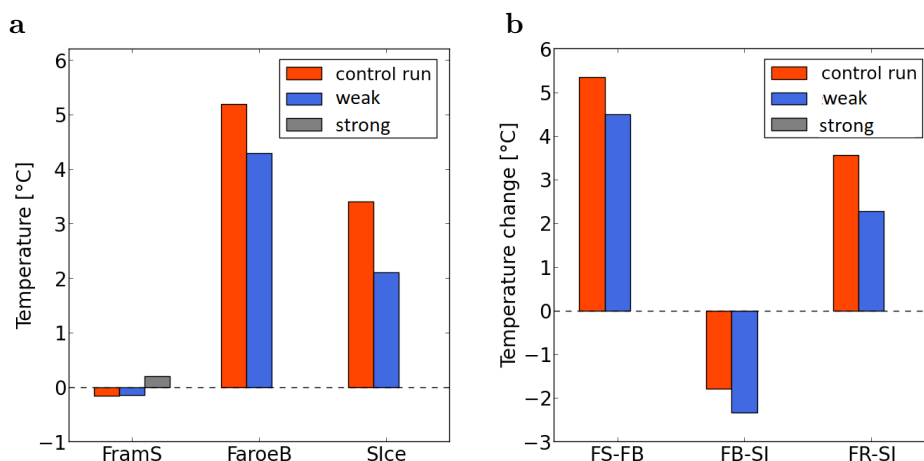


**Figure 5-14:** Mean temperature [°C] of the Arctic waters passing on the east of Iceland into the North Atlantic at three key locations (FramS = Fram Strait, FaroeB = Faroe Bank Channel, Slice = south of Iceland) for the control run, scenario wk and scenario str (a). And temperature changes [°C] between the respective key locations for all three runs (b)

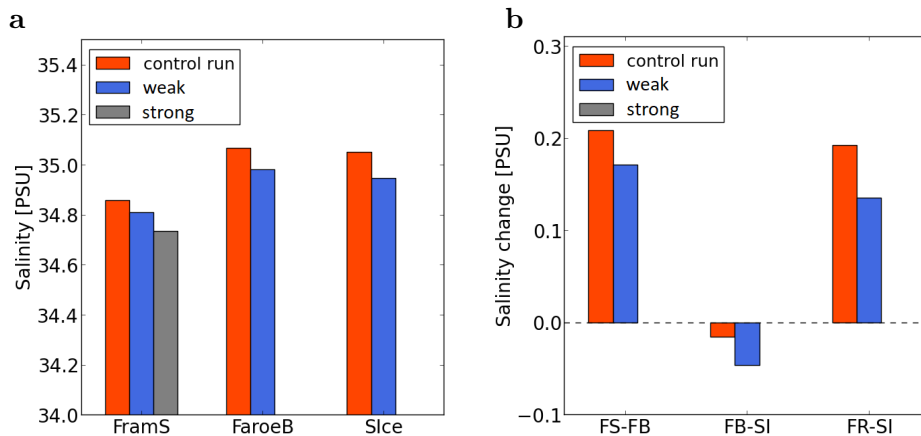


**Figure 5-15:** Mean salinity [ $PSU$ ] of the Arctic waters passing on the east of Iceland into the North Atlantic at three key locations (FramS = Fram Strait, FaroeB = Faroe Bank Channel, Slce = south of Iceland) for the control run, scenario wk and scenario str (a). And salinity changes [ $PSU$ ] between the respective key locations for all three runs (b)

increases to about 0.1 PSU at the Faroe Bank Channel and the south of Iceland. Figure 5-15 b shows the values of absolute change between the key locations for the control run and scenario wk. It shows that the salinity of the particles in scenario wk increase a bit less in salinity between Fram Strait and the Faroe Bank Channel compared to the control run. Subsequently, the scenario wk particles freshen a bit more between the Faroe Bank Channel and the south of Iceland. With values of around 0.02 PSU the difference between the changes are fairly small. Since it was seen that the particles first rise in the water column to cross the Faroe Bank Channel and then sink again (Figure 5-4 d and e), the salinity changes actually act counter that movement. This lets assume that the temperature changes cause the crucial density change which allows the particle cross the channel and subsequently sink again. This is interesting since the runs are only different respective the fresh water input.

# Conclusion and Discussion

This study investigated the pathways of the waters passing Fram Strait. This was done for a present-day climate control run and two scenario runs. The scenario runs are runs equal to the control run but for the increased precipitation over the Arctic Ocean by 50%/300% respectively (scenario wk/scenario str). It was shown in Section 4-1-1 that the extra fresh water input in the Arctic cannot be identified in the EC-Earth model data throughout the whole year by looking at the correlation between the salinity anomaly and the flux anomaly (anomaly between scenarios and the control run). This is due to the sea ice cover which covers the Arctic Ocean most of the year. Therefore, all water passing Fram Strait was traced instead. For transport calculations only southward flow was taken into account in order to prevent double counting. While for scenario wk the absolute transport through Fram Strait increased slightly relative to the control run, for scenario str it decreased by over 20%. It was found that water passing Fram Strait takes four different pathways in the model for an advection time of 20 years: Denmark Strait, Faroe Bank Channel, the Arctic and the Nordic Seas. The pathway through the Faroe Bank Channel ceases to exist for Arctic water in scenario str. The pathways through Denmark Strait and into the Nordic Seas carry most of the Arctic water in all three runs. Notably, the absolute transport into the Nordic Seas remains almost unchanged between all three runs. The absolute transport through Denmark Strait increases for scenario wk and decreases for scenario str relative to the control run. In all three runs the relative share of total transport lies between 40-50%. Almost the entire fresh surface water layer in Fram Strait takes this pathway through Denmark Strait in all three runs. Therefore, the assumptions of van der Sleen (2015) about the fresher Arctic water influencing conditions in the Labrador Sea directly and hence its sinking and convection zones have been confirmed from the Lagrangian viewpoint.

The pathways through Denmark Strait, west of Iceland and the Faroe Bank Channel, east of Iceland have been analysed further as they represent the routes connecting the Arctic with the North Atlantic. In the strong scenario, the Arctic water passing Denmark Strait does no longer form part of the overflow, but is confined to the layers of the upper half of the strait. In general it can be said that the increasing stratification of the Nordic Seas due to net-freshening of the Arctic separates the Nordic Seas from the Denmark Strait pathway. The three key

locations analysed for this route were Fram Strait, Denmark Strait and an area south of the southern tip of Greenland. At all three locations, particles taking this route get fresher with increasing Arctic precipitation. The Arctic water of the weakly forced scenario wk is colder than the control run at all key locations. In contrast, the Arctic water of the strongly forced scenario str is only colder than the control run at Fram Strait and warmer at Denmark Strait and south of Greenland. For all three runs particles of this pathway get warmer from one key location to the next. For the control run and scenario wk, particles freshen slightly in the Nordic Seas and then get more saline after the Denmark Strait. In the strong scenario, particles on this pathways get more saline between all key locations. The waters in Fram Strait stop travelling along the eastern side of Iceland in the strong scenario. Therefore, this pathway could not be analysed further for scenario str. The Fram Strait waters on this route in the control run and in the weak scenario form part of the overflow at Faroe Bank Channel. Temperature and salinity were investigated for three key locations: Fram Strait, the Faroe Bank Channel and an area south of Iceland. For both, the control run and scenario wk, the particles increase their salinity and temperature within the Nordic Seas to then freshen and cool between the Faroe-Bank-Channel and the south of Iceland. The traced waters are fresher and colder for scenario wk at all three locations compared to the control run.

Considering the above results, the Lagrangian approach has proven insightful to further explain changes of ocean circulations in the coupled climate model EC-Earth due to increased precipitation in the Arctic Ocean. However, as could be seen in this study the Eulerian and the Lagrangian approach seem to be most valuable when combined. The Lagrangian approach was used to trace waters in Fram Strait specifically, but the Eulerian approach helps explaining why the respective pathways change with increased Arctic precipitation. A limitation of the Lagrangian approach can be seen for the East Iceland pathway. As shown in Figure 5-2 f, the East Iceland route disappears for scenario str. Needless to say that therefore, the changing properties cannot be analysed of this pathway for scenario str. This illustrates how the Lagrangian approach gives the information about the disappearance of the pathway but it does not give the information as to why this is the case. The Lagrangian approach can only be used to explain change if the pathway exists and changing properties can be compared. In a future study, an attempt could be made to analyse the pathways and properties of those particles in scenario str which do cross the Faroe Bank Channel in the control run and scenario wk. As was shown in Figures 5-3 a and b, the particles of this pathway start for the control run and scenario wk more or less at the same location of Fram Strait. For scenario str these particles stay in the Nordic Seas. The comparison of properties might give further insight as to why the East-Iceland-route disappears. This insight would add to the knowledge of how the increased Arctic precipitation changes ocean circulations.

The results found need to be seen in the light of the methods and tools used. In order to maintain numerical stability, the coupled climate model EC-Earth uses a high viscosity. Hence, the modelled fluid is much more viscous than water. The grid implemented in the model is with  $1^\circ \times 1^\circ$  quite coarse. Therefore, small-scale processes of importance to the large-scale process (e.g. eddies) cannot be resolved. Due to viscosity and resolution, the quality of ocean currents modelled has its limitations. As described in Section 3-1-2 currents like the Gulf Stream are too wide and slightly misplaced. Furthermore, the resolution of the time scale is monthly which is low and therefore decreases accuracy of the results (Qin et al., 2014). At this point in time, models of coarse resolution are commonly used for future climate studies, since higher resolutions are computationally too expensive for century-long

simulations. Yet, this is a state-of-the-art climate model which is able to reproduce the major currents. Whether or not the modelled changes due to increased Arctic precipitation are accurate cannot be verified with measurements at this point in time. However, considering the limited knowledge available combined with the high importance of the matter, results should be given serious attention. In consideration of the limitations mentioned, it can be said that absolute quantities and changes of absolute quantities in this study should be treated with care. However, the general trend and character of change should be taken seriously. Another limitation is the unrealistic aspect of the scenario runs analysed here. The extra precipitation is added by a multiplication factor; hence, it just "appears". Therefore, the water balance is not closed, meaning the ocean gets fuller in the scenario runs. Though this is generally speaking incorrect, this is the best approach available to study the extra fresh water input in the Arctic separately. Furthermore, the model runs are only 50 years long which means the extra water input is very small in relation to the total water mass of the ocean. Therefore, the quality of the results should not be significantly affected by the error made. However, this approach would not be suitable for much longer runs.

In future studies the changes occurring in the Nordic Seas should be analysed more closely. As Figure 5-1 a showed, the amount of transport from Fram Strait into the Nordic Seas remains almost constant for increased Arctic precipitation. In this study the assumption was made that this might be a constant factor which determines how much Arctic water can take other routes. This assumption needs to be scrutinized in further detail. Looking at more scenarios would allow testing whether it can be verified. Whether further supporting evidence can be found for this assumption or not, it is clear that the Nordic Seas play a crucial role in the change of the circulations. Therefore, what happens exactly with the circulations in the Nordic Seas when increasing Arctic precipitation is an important question. This would include analysing the water entering the Nordic Seas from the south and scrutinizing the exchange between the Barents Sea and the Nordic Seas.

Additionally, as could be seen in Figure 5-4 a-c, Arctic water reaching the Labrador Sea through Denmark Strait, sinks after turning around the most southern tip of Greenland. This is also what is known to happen in reality. Van der Sleen (2015) found that the vertical velocities in the Labrador Sea decrease when increasing Arctic precipitation. This study adds the knowledge that the extra precipitation of the Arctic does reach the Labrador Sea, and can thus possibly influence the sinking and convection zones directly. Whether both, sinking and convection zones, are directly affected by the presence of the Arctic water, has not been answered yet. From the results of this study, the quantitative importance of the Arctic water in relation to the total inflow into the Labrador Sea cannot be deduced.

In reality, the current loses buoyancy due to cooling of the boundary current. It is assumed that the model also reproduces the sinking in the Labrador Sea due to cooling. However, in reality the sinking in this region is facilitated by eddies that transport heat from the boundary current into the interior of the Labrador Sea. EC-Earth, however, is not an eddy resolving model, meaning eddies do not influence the model result. And additionally, in contrast to this assumption of a cooling boundary current, Figure 5-10 a and Figure 5-11 a showed that the Arctic waters get warmer and saltier relative to Denmark Strait before sinking in the Labrador Sea. Therefore, the higher salinity could explain the sinking of the Arctic waters, since it increases the density of the water mass. However, this would have to be scrutinized in more detail. As explained in Section 2-1, the sinking within the Labrador Sea is of high importance to maintain the AMOC, and therefore the current climate. Considering the

relevance of the issue, the mechanism of the sinking, and the quantitative influence of the freshening Arctic water should be researched further.

---

# Appendix A

---

## CMS

### A-1 CMS Input files

#### A-1-1 Release File

0000001	335.00	80.00	10.00	1	2027	01	15	0
0000002	335.00	80.00	30.00	1	2027	01	15	0
0000003	335.00	80.00	50.00	1	2027	01	15	0
0000004	335.00	80.00	70.00	1	2027	01	15	0
0000005	335.00	80.00	90.00	1	2027	01	15	0
0000006	335.00	80.00	110.00	1	2027	01	15	0
0000007	335.00	80.00	130.00	1	2027	01	15	0
0000008	335.00	80.00	150.00	1	2027	01	15	0
0000009	335.00	80.00	170.00	1	2027	01	15	0
0000010	335.00	80.00	190.00	1	2027	01	15	0
0000011	335.00	80.00	210.00	1	2027	01	15	0
0000012	335.00	80.00	230.00	1	2027	01	15	0
0000013	335.00	80.00	250.00	1	2027	01	15	0
0000014	335.00	80.00	270.00	1	2027	01	15	0
0000015	335.00	80.00	290.00	1	2027	01	15	0
0000016	335.00	80.00	310.00	1	2027	01	15	0
0000017	335.00	80.00	330.00	1	2027	01	15	0
.								
.								
.								
.								
.								

## A-1-2 Run Configuration

```

&runconf
!=====!
n nests          = 1
timeMax          = 632448000
timestep         = 658800
outputFreq       = 658800
releaseFilename  = "releaseFile"
!=====!
!Turbulence Module
turb             = .false.
horDiff          = 1           !horizontal diffusivity
vertDiff         = 0.1        !vertical diffusivity
turbTimestep     = 3600      !in seconds
!=====!
!Periodic Boundary Condition
periodicbc       = .true.
!=====!
!Landmask Boundary Condition
avoidcoast       = .true.
!=====!
!Backward Tracking Module
backward         = .false.
!=====!
!Output files in ASCII instead of netCDF
ascii            = .false.
!=====!
!Flag for putting particles back in the ocean when they go through the
!uppermost depth level
upperlevelsurface = .true.
!=====!
!Flag for looping through the velocity fields
loopfiles        = .false.
loopfilesstartyear = 69
loopfilesstartmonth = 1
loopfilesstartday = 1
loopfilesendyear = 69
loopfilesendmonth = 1
loopfilesendday = 5
!=====!
!Options for restarting
restartfromfile  = .false.
restartwritefreq = 432000
!=====!
!Options for mixed layer physics
mixedlayerphysics = .false.
mixedlayerwmax   = 0.1
!=====!
&end

```

### A-1-3 Nest input files

```
&nest_input
xaxis= "X"
yaxis= "Y"
zaxis= "Z"
taxis= "T"
zaxis_positive_direction= "down"
tstart_yy=2026
tstart_mm=12
tstart_dd=15
tend_yy=2048
tend_mm=02
tend_dd=15
time_step=2635200
time_units="months"
lon_nameU= "XALT"
lat_nameU= "LAT"
dep_nameU= "DEPTHU"
lon_nameV= "XALT"
lat_nameV= "LAT"
dep_nameV= "DEPTHV"
lon_nameW= "XALT"
lat_nameW= "LAT"
dep_nameW= "DEPTHW"
lon_nameT= "XALT"
lat_nameT= "LAT"
dep_nameT= "DEPTHT"
depth_conversion_factor=1.
time_name= "TCMS"
uvel_name= "U"
vvel_name= "V"
wvel_name= "W"
wvel_positive_direction = "upward"
velocity_conversion_factor=1
dens_name= ""
temp_name= "TEMP"
saln_name= "SAL"
ssh_name= ""
angle_file=""
axorderX = 4
axorderY = 2
axorderZ = 1
axorderT = 3
fill_value=1.e34
agrid=.false.
orthogrid =.true.
$end
```

## A-2 CMS Transport tags

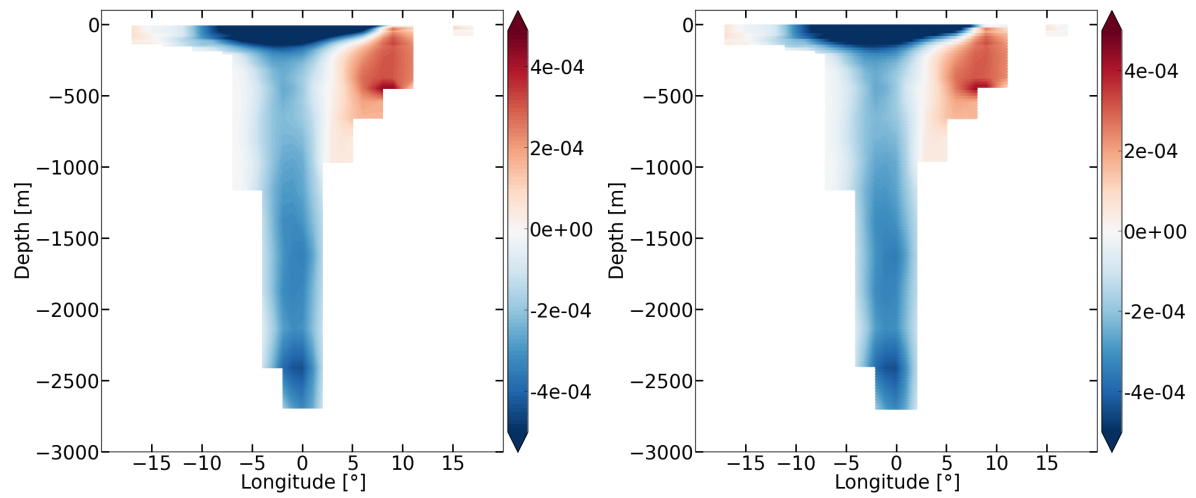


**Figure A-1:** Transport [Sv] at Fram Strait calculated (a) directly from the EC-Earth velocity file and (b) interpolated from the EC-Earth velocity file to the particle position

---

# Bibliography

- Alley, R., Marotzke, J., Nordhaus, W., Overpeck, J., Peteet, D., Pielke, R., Pierrehumbert, R., Rhines, P., Stocker, T., Talley, L., and Wallace, J. (2003). Abrupt climate change. *Science*, 299(5615):2005–2010.
- Balsamo, G., Viterbo, P., Beljaars, A., van den Hurk, B., Hirschi, M., Betts, A. K., and Scipal, K. (2009). A revised hydrology for the ecmwf model: Verification from field site to terrestrial water storage and impact in the integrated forecast system. *Journal of Hydrometeorology*, 10(3):623–643.
- Bintanja, R. and Andry, O. (2017). Towards a rain-dominated arctic. *nature climate change*, 7(4):263–268.
- Bintanja, R., Katsman, C., and Selten, F. (2018). Increased arctic precipitation slows down sea ice melt and surface warming. *Oceanography*, 31(2).
- Bintanja, R. and Selten, F. M. (2014). Future increase in arctic precipitation linked to local evaporation and sea-ice retreat. *Nature*, 509(7501):479–482.
- Fichefet, T. and Marquedá, M. A. M. (1997). Sensitivity of a global sea ice model to the treatment of ice thermodynamics and dynamics. *Journal of Geophysical research*, 102(C6):12,609–12,646.
- Fofonoff, N. and Millard, R. (1983). Algorithms for computation of fundamental properties of seawater. *UNESCO technical papers in Marine Science*, (44).
- Hazeleger, W., Wang, X., Severijns, C., Stefanescu, S., Bintanja, R., Sterl, A., Wyser, K., Semmler, T., Yang, S., van den Hurk, B., van Noije, T., van der Linden, E., and van der Wiel, K. (2012). Ec-earth v2.2: description and validation of a new seamless earth system prediction model. *Climate Dynamics*, 39(11):2611–2629.
- Jackson, L., Kahana, R., Graham, T., Ringer, M., Woollings, T., and an RA Wood, J. M. (2015). Global and european climate impacts of a slowdown of the amoc in a high resolution gcm. *Climate Dynamics*, 45(11-12):3299–3316.

- Kanzow, T., Cunningham, S. A., Johns, W. E., Hirschi, J. J.-M., Marotzke, J., Baringer, M. O., Meinen, C. S., Chidichimo, M. P., Atkinson, C., Beal, L. M., Bryden, H. L., and Collins, J. (2010). Seasonal variability of the atlantic meridional overturning circulation at 26.5°N. *Journal of Climate*, 23(21):5678–5698.
- Katsman, C. (2016). In Pietrzak, J., editor, *An Introduction to Oceanography for Civil and Offshore Engineers*, chapter Thermohaline Circulation, pages 155–172. Environmental Fluid Mechanics Section - Department of Hydraulic Engineering TU Delft.
- Katsman, C., van der Sleen, N., Bintanja, R., Selten, F., Wijnberg, K., and Hulscher, S. (2018). *Impacts of Arctic precipitation changes on the Atlantic Meridional Overturning Circulation*. paper in preparation for the Journal of Geophysical Research Oceans.
- Kolb, P. and Riahi, K. (2009). Rcp database (version 2.0). Available from [http://www.ec-earth.org/images/sc\\_i\\_plan\\_ec-earth.pdf](http://www.ec-earth.org/images/sc_i_plan_ec-earth.pdf). Last accessed on Oct 24, 2017.
- Madec, G. (2016). Nemo ocean engine. *Note du Pole de modélisation, Institut Pierre-Simon Laplace (IPSL), France*, (27).
- Millero, F. and Poisson, A. (1981). International one-atmosphere equation of state of seawater. *Deep Sea Research*, 28A(6):625–629.
- Olbers, D., Willebrand, J., and Eden, C. (2012). *Ocean Dynamics*. Springer-Verlag.
- Paris, C. B., Vaz, A. C., Helgers, J., Wood, S., and Ross, R. (2017). Connectivity modeling system: User’s guide cms v2.2. Available from <https://github.com/beatrixparis/connectivity-modeling-system/blob/master/User-Guide-v2.pdf>. Last accessed on Oct 25, 2017.
- Perkins, H. and Hopkins, T. (1998). Oceanographic conditions east of iceland. *Journal of Geophysical Research*, 103(C10):21531–21542.
- Qin, X., van Sebille, E., and Gupta, A. S. (2014). Quantification of errors induced by temporal resolution on lagrangian particles in an eddy-resolving model. *Ocean Modelling*, 76:20–30.
- Rahmstorf, S. (2001). In Steele, J., editor, *Encyclopedia of Ocean Sciences*, chapter Abrupt Change, pages 1–6. Academic Press.
- Rahmstorf, S. (2007). In Elias, S., editor, *Encyclopedia of Quaternary Science*, chapter Thermohaline Ocean Circulation, pages 739–750. Elsevier.
- Sterl, A., Bintanja, R., Brodeau, L., Gleeson, E., Koenigk, T., Schmith, T., Semmler, T., Severijns, C., Wyserr, K., and Yang, S. (2012). A look at the ocean in the ec-earth climate model. *Climate Dynamics*, 39(11):2631–2657.
- Stommel, H. (1961). Thermohaline convection with two stable regimes of flow. *Tellus*, 13(2):224–230.
- Talley, L., Pickard, G., Emery, W., and Swift, J. (2011). *Descriptive Physical Oceanography: An Introduction*. Elsevier.
- Toggweiler, J. and Key, R. (2003). In Steele, J., editor, *Encyclopedia of Ocean Sciences*, chapter Thermohaline Circulation, pages 2941–2947. Academic Press.

Valcke, S. (2006). *PRISM An Infrastructure Project for Climate Research in Europe: OASIS3 User Guide*.

van der Sleen, N. (2015). The effect of arctic precipitation changes on the atlantic meridional overturning circulation. *University Twente and KNMI*.



---

# Acronym

AMOC	Atlantic Meridional Overturning Circulation
CMS	Connectivity Modelling System
SV	Sverdrup - equal to $10^6 \frac{m^3}{s}$
THC	Thermohaline Circulation

